UNIVERSITY OF ALBERTA

BIOLOGICAL RESPONSES OF TUMOUR CELLS TO FREEZING USING A NOVEL CRYOSURGICAL MODEL SYSTEM

by

Christine Elsa Humphreys ©

A thesis submitted to the Faculty of Graduate Studies and Research in partial fulfillment of the requirements for the degree of Master of Science

in

Experimental Pathology

Department of Laboratory Medicine and Pathology

Edmonton, Alberta

Spring 1999

National Library of Canada
Acquisitions and Bibliographic Services
395 Wellington Street
Ottawa ON K1A 0N4
Canada

Bibliothèque nationale du Canada
Acquisitions et services bibliographiques
395, rue Wellington
Ottawa ON K1A 0N4
Canada

Your file Votre référence

Our file Notre référence

The author has granted a non-exclusive licence allowing the National Library of Canada to reproduce, loan, distribute or sell copies of this thesis in microform, paper or electronic formats.

The author retains ownership of the copyright in this thesis. Neither the thesis nor substantial extracts from it may be printed or otherwise reproduced without the author's permission.

L'auteur a accordé une licence non exclusive permettant à la Bibliothèque nationale du Canada de reproduire, prêter, distribuer ou vendre des copies de cette thèse sous la forme de microfiche/film, de reproduction sur papier ou sur format électronique.

L'auteur conserve la propriété du droit d'auteur qui protège cette thèse. Ni la thèse ni des extraits substantiels de celle-ci ne doivent être imprimés ou autrement reproduits sans son autorisation.

0-612-40061-1

Canada

UNIVERSITY OF ALBERTA

LIBRARY RELEASE FORM

Name of Author:	**Christine Elsa Humphreys**
Title of Thesis:	**Biological Responses of Tumour Cells to Freezing Using a Novel Cryosurgical Model System**
Degree:	**Master of Science**
Year this Degree Granted:	**1999**

Permission is hereby granted to the University of Alberta Library to reproduce single copies of this thesis and to lend or sell such copies for private, scholarly or scientific research purposes only.

The author reserves all other publication and other rights in association with the copyright in the thesis, and except as hereinbefore provided, neither the thesis nor any substantial portion thereof may be printed or otherwise reproduced in any material form whatever without the author's prior written permission.

Christine Elsa Humphreys

10756 81 Avenue #205
Edmonton, Alberta
T6E 1Y3

Jan 22, 99

UNIVERSITY OF ALBERTA

FACULTY OF GRADUATE STUDIES AND RESEARCH

The undersigned certify that they have read, and recommended to the Faculty of Graduate Studies and Research for acceptance, a thesis entitled **Biological Responses of Tumour Cells to Freezing Using a Novel Cryosurgical Model System** submitted by **Christine Elsa Humphreys** in partial fulfillment of the requirements for the degree of **Master of Science** in **Experimental Pathology**.

Dr. Locksley McGann (supervisor)

Dr. M. Jean Turner

Janet Elliott

Dr. Janet Elliott

Dr. Kim Solez

21 January 1999

Date

This thesis is dedicated to my parents for their love, support, encouragement and belief in me. I would not be where I am today without them.

ABSTRACT

A novel cryosurgical model system is developed that allows physical and thermal measurements to be correlated with biological outcomes to better understand cellular responses to freezing and ice-ball dynamics. A realistic model system is designed, biological assessment techniques validated and biological freeze-thaw experiments performed and analysed. Cell viability is evaluated using fluorescent stain Syto/EB and metabolic assay alamarBlue after subjecting cells to a single or double freeze-thaw cycle, or freeze cycling. The effects of cooling rate, end temperature, number of cycles, and temperature cycling are investigated, resulting in the double freeze-thaw protocol being the most effective at killing cells. At regions closest to the probe, increased cooling rates and repeated freezes are most important in cell death. In the periphery where cells survive, complete thawing and increased cycle numbers are necessary. Since increases above two freeze-thaw cycles lead to severe complications, adjuvants to increase cell death are necessary in addition to cryosurgery.

ACKNOWLEDGEMENTS

I would like to acknowledge the following people for their help with this thesis:

To Dr. Locksley McGann my supervisor, I would like to express my gratitude for your guidance and inspiration on this journey.

To Dr. Rick Batycky and Mr. Rod Gonzales for help with theoretical aspects of this thesis.

To Dr. Joan Turner for serving as a committee member, your helpful suggestions, and donation of the cell lines.

To Dr. Janet Elliott for serving as a committee member, your interest and review of this thesis is appreciated.

To Dr. Kim Solez for serving as chairman of my supervisory committee.

To Jason for his love, support, patience, and belief in me. Words can not express how loved and cherished you truly are.

TABLE OF CONTENTS

CHAPTER			PAGE
1.	INTRODUCTION AND LITERATURE REVIEW		
	1.1	Development of Cryosurgery	1
	1.2	Cryobiology of Single Cells	3
	1.3	Cryobiology of Tissues	8
	1.4	Current Cryosurgical Procedures	11
	1.5	Objectives	13
	1.6	References	18
2.	DEVELOPMENT OF A CRYOSURGICAL MODEL SYSTEM		
	2.1	Introduction	23
		Rationale	24
		Objectives	24
	2.2	Materials	25
		Cryosurgical Model System Design	25
		Cell Culture	27
		Experimental Medium	28
		Assessment of Membrane Integrity	29
		Metabolic assay	30
	2.3	Methods	30
		Cryosurgical Model System Function	30
		Determination of Optimal Media and Membrane-Integrity	31
		Metabolic Assay	33
	2.4	Results	34
		Cryosurgical Model System Function	34
		Cell Line Choice	35
		Optimal Freezing Medium and Syto/EB	36
		Metabolic Assay	37

	2.5	Discussion	38
		Cryosurgical Model System	38
		Medium	42
		Assessment Techniques	45
	2.6	References	47
3.	BIOLOGICAL RESPONSES TO SINGLE AND DOUBLE FREEZE		
	3.1	Introduction	62
	3.2	Materials and Methods	65
		Cell Culture	65
		Media Preparation	66
		Cryosurgical System and Freezing Protocols	66
		Syto/EB	67
		AlamarBlue	67
	3.3	Results	68
		System Function	68
		Syto/EB	69
		AlamarBlue	70
		Cooling Rate and End Temperature Effects	70
	3.4	Discussion	71
	3.5	References	77
4.	BIOLOGICAL RESPONSES TO TEMPERATURE CYCLING		
	4.1	Introduction	91
	4.2	Methods and Materials	93
		Cell Culture	93
		Media Preparation	93
		Cryosurgical System and Freezing Protocols	94
		Syto/EB	95
		AlamarBlue	95
	4.3	Results	96
		System Function	96

Syto/EB 96
AlamarBlue 97
Cooling Rate and End Temperature 98
4.4 Discussion 98
4.5 References 103

5. GENERAL DISCUSSION AND CONCLUSION

5.1 Review of Thesis Objectives 117
5.2 Summary of Results 117
5.3 Significance to Cryosurgery 119

APPENDIX A

A.1 Introduction 120
Steady State Ice Front Prediction 121
Transient: Unsteady State Single Phase 123
A.2 Methods and Materials 123
A.3 Results 125
A.4 Discussion 126
A.5 References 128

APPENDIX B

B.1 General Discussion 133
B.2 References 135

LIST OF TABLES

		PAGE
Table 2.1	Gel Concentration versus Distance Cells Travel	60
Table 2.2	Comparison of Membrane Integrity in Degassed and Non-degassed Methocel	61
Table 3.1	Comparison of Syto/EB Results for the Single and Double Freeze-thaw Protocols	88
Table 3.2	Cell Death versus Cooling Rate and Temperature for Single Freeze-thaw Protocol	89
Table 3.3	Cell Death versus Cooling Rate and End Temperatures for the Double Freeze-thaw Protocol	90
Table 4.1	Comparison of Syto/EB Results for the Double and Triple Freeze Cycle Protocols	112
Table 4.2	Cell Death versus Cooling Rate for the Double Freeze Cycle Protocol	113
Table 4.3	Cell Death versus Cooling Rate for the Triple Freeze Cycle Protocol	114
Table 4.4	Cell Death versus End Temperature in the Double Freeze Cycle Protocol	115
Table 4.5	Cell Death versus End Temperature in the Triple Freeze Cycle Protocol	116

LIST OF FIGURES

		PAGE
Figure 2.1	Cryosurgical Model System Picture	51
Figure 2.2	Schematic of Cryosurgical Model System Viewed from the Top	52
Figure 2.3	Schematic of Cryosurgical System Set Up	53
Figure 2.4	Schematic of Methocel Concentration Experiments	54
Figure 2.5	Water Freeze Temperature Profiles	55
Figure 2.6	PBS Freeze Temperature Profiles	56
Figure 2.7	Methocel Freeze Temperature Profiles	57
Figure 2.8	Ice-ball Growth versus Time	58
Figure 2.9	Percent AlamarBlue Reduced versus Cell Concentration	59
Figure 3.1	Single Freeze-thaw Temperature Profiles	81
Figure 3.2	Double Freeze-thaw Temperature Profiles	82
Figure 3.3	Single Freeze-thaw Membrane Integrity	83
Figure 3.4	Double Freeze-thaw Membrane Integrity	84
Figure 3.5	Comparison of Cell Viability for Single and Double Freeze-thaw Using AlamarBlue	85
Figure 3.6	Comparison of AlamarBlue versus Syto/EB Results for Single Freeze-thaw	86
Figure 3.7	Comparison of AlamarBlue versus Syto/EB Results for Double Freeze-thaw	87
Figure 4.1	Double Freeze Cycle Temperature Profiles	105
Figure 4.2	Triple Freeze Cycle Temperature Profiles	106
Figure 4.3	Membrane Integrity of Cells in the Double Freeze Cycle Protocol	107

PAGE

Figure 4.4 Membrane Integrity of Cells in the Triple Freeze Cycle Protocol 108

Figure 4.5 Cell Viability using AlamarBlue for the Double and Triple Freeze Cycles 109

Figure 4.6 Comparison of Syto/EB versus AlamarBlue Results for the Double Freeze Cycle Protocol 110

Figure 4.7 Comparison of AlamarBlue and Syto/EB Results for the Triple Freeze Cycle 111

Figure A.1 Schematic of the Cryosurgical Model System 129

Figure A.2 Theoretical Plot of Temperature versus Time for Different Radial Distances from the Probe 130

Figure A.3 Comparison of Theoretical and Experimental Thermal Profiles 131

Figure A.4 Comparison of Theoretical versus Experimental Ice-ball Radii 132

LIST OF ABBREVIATIONS

ABBREVIATIONS

CO_2	carbon dioxide
EB	ethidium bromide
methocel	methylcellulose
PBS	phosphate buffered saline
UV	ultraviolet

CHAPTER 1: INTRODUCTION AND LITERATURE REVIEW

1.1 Development of Cryosurgery

The treatment of disease by application of cold or cryotherapy dates back thousands of years, mostly for treatment of pain, swelling and bleeding. The first application of sub-zero temperatures in the treatment of tumours was employed by Sir James Arnott in the treatment of malignancies through the use of cold brine solutions (1). This treatment was not particularly effective at eradicating the tumour, although it reduced both its size and discharge. The next enormous strides forward in the evolution of cryotherapy occurred in the late 1800's with the liquefaction of gasses including oxygen and nitrogen (2). Dewar's invention of the vacuum flask in 1898 allowed for storage of liquefied gasses and the birth of cryosurgery (3).

Cryosurgery is the use of controlled localized freezing to selectively destroy undesired tissues. The first cryosurgeons used cotton dipped applicators and spray bottles to treat benign, precancerous, and cancerous lesions of the skin (4,5,6,7). Cryosurgery as we know it is possible due to Irving Cooper who invented the first closed cryoprobe system that circulates liquid nitrogen through a sealed metal tube. Cooper used this method in the treatment of Parkinson's Disease by placing the probe in contact with the area of the tissue to be frozen (8). Cryosurgery is extensively accepted and used in dermatology, as it is a highly effective treatment for many afflictions from benign lesions such as scarring and warts, to premalignant and malignant diseases like lentigo maligna and basal cell

carcinoma (9,10). It is also used successfully in ophthalmology, gynecology, neurosurgery, and cardiology (10).

There is considerable interest in cryosurgery since it has many advantages over that of traditional cancer treatments. These benefits include the facts that: resection of large volumes of normal tissue surrounding the tumour is unnecessary, tumours located next to large blood vessels can be safely treated since the vessels can tolerate freezing well, cryosurgery is a focal treatment and specific areas can be targeted, recurrence of disease can be retreated, blood loss is minimized, and the patient's immune system may be sensitized to tumor antigens (11).

Beginning in the late 1960's, cryosurgical treatment of benign prostatic hyperplasia and prostate cancer by transurethral cryoprostatectomy got its start (12). The rate of complications was very high due to technical problems during surgery, including the inability to monitor temperature, size and location of the ice-ball. Due to these obstacles, routine cryosurgery of tumours in the visceral organs was discontinued until the development of novel imaging techniques. Intraoperative and transrectal ultrasound revolutionized cryosurgery and brought it into the modern era by enabling better placement of probes, thermocouples, and monitoring the extent of freezing (13).

Today, cryosurgery is used with increasing frequency for the treatment of liver and prostate cancer, but recurrence of disease after therapy is still problematic (12,14,15,16). In many cases it is assumed that the radius of freeze is also the radius of kill. This is presumed since there are clear differences between

the frozen and unfrozen tissue sections after thaw, which is interpreted as healthy or dead tissue respectively. Recurrence of malignancy leads one to the assumption that either the entire tumour was not frozen during the cryosurgical procedure or that some tumour cells survive the freezing process. Many surgeons will freeze 1 cm outside the tumour margin especially in liver cryosurgery. Reoccurrence of the neoplasm happens in many patients (14,15,17). Therefore, current cryosurgical procedures are inadequate and vital information about tumour cell responses to freezing is lacking. The current limitations to cryosurgery as a therapeutic tool include the ability of some neoplastic cells to survive low sub-zero temperatures and a lack of predictability of outcome. This points to the need for better understanding of cell and tissue responses during cryotherapy if it is to become a reliable alternative to current cancer treatments.

1.2 Cryobiology of Single Cells

One of the most interesting paradoxes in cryobiology is that cells can either be preserved or destroyed by the freezing process. Understanding the events that occur during freezing, the physical and biological responses of cells, helps us to comprehend why cells live or die at low temperatures. As cells are slowly cooled to temperatures below 0°C, extracellular ice begins to form in the external medium while the interior of the cell remains unfrozen. Upon ice forming outside the cell, water is removed from the extracellular solution in the form of ice, solutes are excluded, and an increase in extracellular solutes in the unfrozen fraction results. The water inside the cell has a higher chemical potential than the water of the extracellular solution. As a result of the difference in chemical potential, water will

flow out of the cell by exosmosis provided that the rate of cooling is sufficiently slow. This enables the cell to maintain osmotic equilibrium with its environment. The cell will become increasingly dehydrated upon continued cooling and if the cooling rate is sufficiently slow will not freeze intracellularly.

Cooling cells rapidly results in the formation of intracellular ice. The probability of intracellular ice formation in a given cell is a function of the cooling rate and volume of the cell (18,19). If the rate of cooling is rapid, then the cell can not lose water swiftly enough to maintain osmotic equilibrium. The interior of the cell becomes supercooled resulting in intracellular freezing.

Mazur, Leibo and Chu provided an explanation for the causes of injury to rapidly and slowly cooled cells in their two-factor hypothesis of freezing injury in 1972 (20). This study was initiated by the presence of an optimum cooling rate, above and below which cells were found to be damaged. This suggested that cell survival is affected by two classes of factors, which are conversely dependent upon cooling rate. The first factor involves changes in the intracellular and extracellular solutions as a result of ice formation, when the solution in the interior of the cell becomes increasingly hypertonic. The injurious effect of these changes increases with decreasing cooling velocities. Injury is a consequence of the lengthy duration of exposure to high concentrations of solutes that can affect cell structure and function. Alternatively, damage from rapid cooling rates results from intracellular ice formation, and recrystallization during slow warming.

Damage occurring during slow cooling is thought to happen three different ways; deleterious solute concentrations (20), deviation below minimum critical

volumes (21), and alterations to cell membrane surface area (22). In the first case, cells lose cytoplasmic water to the exterior of the cell and ice is formed extracellularly. This causes an increase in the intracellular concentration of solutes that may be toxic to cells, change the pH, or causes the precipitation of solutes (20). Precisely what happens on a molecular level to damage cells as a result of solute concentration remains unknown.

Cell volume reduction by osmosis is another method by which cells are thought to be injured during slow cooling (21). The exact mechanism by which volume decrease damages cells is unknown, although it has been postulated that there is a mechanical resistance to shrinkage. Evidence exists to suggest that there is a minimum critical volume below which the cell can not deviate.

Wiest and Steponkus have proposed that the surface area of a cell is reduced during the dehydration of slow cooling (22). When the cell is restored to isotonic volume during thawing, the cell becomes damaged when it exceeds its decreased surface area.

The second factor in cell injury during freezing is due to the fact that cooling cells rapidly results in the formation of intracellular ice. As cooling progresses, the interior of the cell becomes supercooled. The cell can not lose water swiftly enough to maintain osmotic equilibrium. As a consequence of disequilibrium the cell freezes intracellularly. It is thought that the cell membrane itself presents a barrier to ice propagation (23), so other mechanisms of intracellular ice nucleation within a cell must be at play.

The first theory of intracellular ice nucleation proposed by Levitt, who hypothesizes that cells nucleate spontaneously at an exact amount of supercooling (24), where supercooling is defined as the difference between freezing point and the actual temperature of the cell.

Mazur's theory states that intracellular ice forms when the cytoplasm is nucleated through aqueous pores in the plasma membrane (20). When the tip of a growing ice crystal is equal to the size of the pores, the extracellular ice propagates through the membrane resulting in the nucleation of intracellular water.

Other theories state that membrane damage leads to the formation of intracellular ice. One such theory promotes intracellular ice nucleation due to electrical transients at the ice interface (25). When electrical transients reach a critical level, they rupture the plasma membrane and allow intracellular ice nucleation. Another theory by Toner includes the idea that intracellular ice could be formed if the membrane acted as a nucleator of intracellular ice when it was acted upon by extracellular ice (26). Another possible explanation is posed by the osmotic rupture hypothesis, which states that at some critical gradient in osmotic pressure, the membrane is damaged (27). As a result of this injury intracellular ice formation occurs.

Regardless of how intracellular ice forms within a cell, it is thought to be lethal to cells since the cooling rates that produce intracellular ice also cause enormous amounts of cell death (19). The exact mechanism of damage is not known, however it is postulated that injury from intracellular ice formation may be due to mechanical forces from the ice on the plasma and intracellular organelle

membranes. Other non-mechanical types of damage may include gas bubble formation from the intracellular ice (28) and osmotic effects produced during melting of intracellular ice (29).

Evidence shows that some cells that form intracellular ice survive if warmed very rapidly (18,19,20). The ice crystals that form during rapid cooling tend to be very small. These small crystals are inclined to be less thermodynamically stable in comparison to larger crystals and have a tendency to form large crystals upon slow warming (18,19,20). Slow warming with recrystallization is extremely harmful to cells. It can be more harmful than the formation of intracellular ice (18,19,20). If some of those cells that contain intracellular ice crystals are warmed at a fast enough rate, the ice crystals melt before recrystallization can damage the cells. Others think that it is not the formation of intracellular ice or its recrystallization *per se* that damages cells, but the amount or location within the cell.

Cells within a cryosurgical ice-ball will undergo a myriad of cooling rates. Cells closest to the probe will experience the fastest rate of cooling, while those cells in the outer segment of the ice-ball will encounter the slowest rate of cooling. Information on cellular cryobiology is very important in understanding the responses of tumour cells to freezing. This thesis will examine the thermal histories of cancer cells and how they relate to cell kill or outcome. I hypothesize that manipulation of freezing protocols will allow increased amounts of tumour cell kill that will be useful in improving current cryosurgery techniques.

1.3 Cryobiology of Tissues

Tissues are comprised of many cells and different cell types, which makes them more complex than single isolated cells. The kind of damage that occurs in single cells in suspension as a result of the freezing process also damages individual cells in a tissue system, however evidence exists to show that the responses of cells to freezing are altered depending on whether or not they are individual cells or an element in tissue (30). Another significant difference between single cells and tissues is the sheer difference in size. The scale of the tissues introduces the concepts of heat and mass transfer, as well as tissue specific modes of damage.

When a tissue is frozen, the direction of freeze proceeds from the surface of the tissue in contact with the cryoprobe towards the outer tissue in the direction of the temperature gradient. Experiments show that once ice forms in the vasculature, it follows the path of least resistance and propagates through the vascular system since there are no barriers to halt ice formation (31,32). The architecture of the vascular system remains intact as continuous ice crystals form along the vasculature. Assuming that the cell membrane is impervious to ice, ice will grow in the direction of temperature gradient, particularly in the blood vessel pathway.

At slow rates of cooling, the probability of intracellular ice formation is low. Therefore the cells adjacent to the blood vessels do not form intracellular ice (31,32). As ice forms in the vasculature, water is removed from solution, solutes are excluded from the forming ice, and the remaining solution becomes

hypertonic. The concentration differences between the remaining hypertonic solution in the vessel and the cells surrounding the vessel induces the cells to dehydrate, losing water into the vasculature. Experiments show that the water entering the vasculature is subsequently frozen, expanding the vessel's size. This expansion is thought to cause a loss of functional integrity as the vessels overdistend and rupture. Other studies show that blood vessel flow returns immediately post thaw, accumulating damage to the vessel walls (33). After many hours, platelet thrombi form and cessation of flow occurs. The resulting ischemia contributes significantly to cell death.

At higher rates of cooling, the cells surrounding the vasculature are supercooled and do not dehydrate significantly, and intracellular ice forms in these cells. (31,32). The appearance of rapidly frozen tissue is characterized by the appearance of multiple small intracellular ice crystals (34,35). The location and shape of the ice crystals depends on different factors including the rate of cooling, presence of blood supply, nature of the tissue, and location within the cell (cytoplasm or nucleus) (35). Upon thawing rapidly cooled samples there is disruption of the stroma with the appearance of numerous small tears, epithelial cells became completely detached, and the nuclei are distorted (34). Experimental evidence from both slow and fast cooling demonstrates that cells suffer microscopic cellular damage from solution effects and intracellular ice. The presence of damaged blood vessels also causes macroscopic injury. This helps to explain why more cell death occurs in tissue than in isolated cells.

Other differences between single cells in suspension and tissues are the presence of cell-cell and cell-matrix interactions. Experimental evidence shows that many cell types including rat hepatocytes, bovine corneal endothelial cells, and hamster fibroblasts all form intracellular ice at lower rates of cooling and higher temperatures (30). These junctional interactions may be responsible for the differences seen between isolated and cultured cells.

Heat and mass transfer processes are other means by which tissues and single cells can be differentiated. Mass transport in cryosurgery refers to the redistribution of water during the freezing and thawing process. In single cells the semipermeable membrane limits water transport. In tissues one must consider cell-cell and cell-interstitium transport (30). In the periphery of the ice-ball cells dehydrate at a slower rate than those closer to the probe as a result of slow cooling rates.

Heat transfer processes are also present due to the macroscopic size of the tissue. The cryoprobe is thought of as a heat sink as heat flows by conduction from the tissues to the cryoprobe. There is the presence of large thermal gradients between the interior and exterior of the ice-ball, which imply non-uniform cooling rates (34). The cells at the interior of the ice-ball will encounter more rapid rates of cooling and be subjected to lower temperatures, while those cells within the exterior portion of the ice-ball encounter slower rates of cooling at higher temperatures.

We need to acknowledge the differences between single cell and tissue freezing processes before proceeding with cryosurgery research. Knowing the

effects of cooling rate, temperature, and effects due to the macroscopic size of the tissue helps to understand how they may affect tumour cell responses to freezing. This information provides insight into ways of maximizing damage to tumour cells during cryosurgery.

1.4 Current Cryosurgical Procedures

Cryosurgery is a successful treatment for many diseases, but is most commonly used for lesions located on the surface of tissues that are easily accessible. The two most significant areas in cryosurgery where improvement is necessary are in prostate and liver cryoablation. These deep organs are difficult to freeze due to their location and the inability to accurately judge the amounts of kill within the ice-ball. In prostate cancer cryotherapy, the most common approach to surgery involves the use of five probes inserted percutaneously into the prostate (16,36,37,38). The amount of freezing is limited by the geography of the prostate and surrounding tissue. The surgeon does not want to freeze the rectum or bladder neck for fear of serious complications; however sufficient freezing must occur in order to completely destroy all tumour cells (36). The avoidance of serious complications takes precedence over the actual degree of freezing when patient treatment is considered. Temperatures are measured by thermocouples inserted into various places within the prostate and are used to monitor freezing along with ultrasound. The duration of freeze varies, but in some reports was estimated to last 5 to 15 minutes (12,37,38). In most cases a second freeze was performed to ensure sufficient tissue destruction. In some surgeries the tissue was completely thawed (38), and in others, the tissue was warmed to a specific sub-zero

temperature without completely thawing (12,37). The double freeze with complete thaw kills more cells, but can lead to more post-operative complications (12). Therefore, the double freeze without complete thaw is used in some cases since it causes more damage than a single freeze-thaw, but decreases the rate of complications.

In liver cryosurgery the freezing process is similar. The number and placement of probes depends on the size and number of tumours, therefore no standard exists. The amount of freezing depends both on the size of the tumour and how much normal tissue is destroyed in the tumour margin. Most surgeons recommend freezing no greater a tumour diameter than 3-5 cm, since recurrence of malignancy is common (11,17). In most cases a 1-cm tumour margin of normal hepatic tissue is frozen (14,17) and a double freeze-thaw cycle is used.

Some surgeons use a double freeze with partial thaw, as it is better tolerated by patients (14). Earlier in liver cryosurgery history, a phenomenon known as cryoshock devastated some patients with severe complications including death. Experimental evidence suggests that there is an increased amount of hepatocellular injury, which may eventually lead to multisystem organ failure (17). For these reasons, recommended practice is the modified double freeze with partial thaw.

Since a high majority of liver tumours are not resectable, cryosurgery becomes an extremely valuable tool in the treatment of non-resectable liver cancer (15,17). A single tumour that is located next to blood supplies, in anatomically difficult locations such as near the bile duct, or multiple tumours, that can not be

resected, are now targeted for treatment (11). Also, when hepatic reserve can not be removed due to cirrhosis or a co-morbid condition exists such as a cardiopulmonary problem that precludes resection, cryosurgery can still be performed.

Many problems exist with current cryosurgical techniques. There are difficulties freezing deep tissues due to their location and the inability to accurately judge the amounts of kill within the ice-ball. Much of cryosurgery is performed based on qualitative observations made during the procedure, and a cure is not possible in many cases. A more scientific approach to cryosurgery is necessary to better understand the responses of tumor cells to freezing and dynamics occurring within the ice-ball. This, in turn, will be clinically relevant when applied to improving treatment planning of cryosurgical procedures.

1.5 Objectives

Many of the current cryosurgical procedures are performed based on qualitative observations and scientific evidence provided by limited studies. These studies are all based upon the facts that rapid cooling, along with slow warming, and multiple freeze thaw regimens are the most damaging to single cells in suspension. Surely, the most important indicator of complete tumour cell necrosis would be evident from the lack of tumour recurrence. However, many studies of cryosurgery do not evaluate long-term results. So if recurrence of disease is not an easily obtainable measure of outcome, one must question what happens to the individual cells within the tissue at various distances from the cryoprobe. To make cryosurgery more successful, surgeons need basic information about thermal

histories and how they relate to outcome. It will become necessary to develop specific optimal protocols that have been experimentally proven to work and are based on sound scientific evidence applicable to cryosurgery. To be able to realize these goals, we need to develop ways to study the responses of cells in a controlled manner.

The main objective of this research is a better understanding of the biological responses of tumour cells to freezing during cryosurgery. The tactics involved include; building a realistic cryosurgical model system that allows assessment of cryosurgical procedures, determination of adequate biological assessment techniques of the cells after freezing, and the performance and analysis of freeze-thaw biological response experiments. The hypothesis is that this model system will permit correlation of physical and thermal measurements with biological outcomes, to assess and increase the efficiency of different cryotherapeutic protocols.

The first specific objective of this research consists of building a cryosurgical model system such that it is a physically realistic model of cryosurgery with simple geometry, and has well-defined boundary conditions. Secondly, the model should permit the assessment of cryosurgical procedures in a defined environment, to be able to characterize more effective freeze-thaw protocols. It should also be possible to model both thermal and biological responses, as well as measure temperature distribution and ice-ball size as a function of time. As a result, the system will allow correlation of thermal profiles and freezing conditions with biological outcomes.

Tissues are very complex systems that consist of many cells and cell types. To simplify this and study the individual cells within a tissue is the second objective. Different media are tested to determine immobilization of cells, maintenance of media structure after freezing, toxicity, and compatibility with assessment techniques.

In order to determine the responses of cells to freezing it is important that the viability assessment techniques be compatible with the system. I will use alamarBlue, a new metabolic assay that will be evaluated for assessment of metabolic function by the cells ability to reduce the dye from its oxidized to reduced form and measure cell viability (39). The concentration of cells, compatibility with the gel and incubation times necessary for the experiments to work will be determined. Syto/Ethidium bromide (EB) will be the second method investigated for compatibility with the system. This is a membrane integrity assay that distinguishes cells by the presence or absence of intact membranes (40). Both assays will be used since one imparts information about membrane integrity, not information as to whether or not the cells are still functioning. AlamarBlue is dependent upon enzyme activity that gives information about cell viability.

The level of knowledge concerning tumour cell response to freezing is inadequate. Cryosurgeons often assess amounts of cell kill based upon the area frozen, where the ice-ball radius equals the zone of kill. The objectives of the next set of experiments will be to determine the biological responses of these cells within the cryosurgical model system. The first objective, before

experimentation, is to have validated a theoretical description of the system by experiments based on the known properties of water. The experiments were performed by myself but mathematically validated by Mr. Rod Gonzales and Dr. Rick Batycky of the Chemical Engineering Department and are added as an appendix in this thesis since my main study is on the biological aspects of cryosurgery. Once the system function is documented, experiments with a physiological salt solution and a gel will be compared in order to monitor the thermodynamics of the system and document any differences.

The ability to determine biological responses of cancer cells to a single freeze-thaw cycle will be examined at a probe temperature of –196°C, as the first step towards establishing measurable biological outcomes under specific freezing conditions. This will create a scale of cell kill at a given radius and treatment time.

It is widely accepted that double freeze-thaw cycles enhance the amount of damage to cells. I will examine the effects of multiple freeze-thaw cycles to determine the variation in cell kill dependent upon the number of freeze-thaw cycles, according to radius. This will involve altering the number of freeze-thaw cycles and the amount of time at sub-zero temperatures, since increasing the time at sub-zero temperatures has been shown to decrease cell viability.

One other objective is to examine the effects of temperature cycling without complete thawing on cellular viability as a function of radial distance from the probe. As a result of cycling temperatures, there will be changes in both temperature and water distribution within the ice-ball. Some hypothesize that cycling temperatures will create osmotic stresses within the ice-ball that are

damaging to cells (37). I will experiment with different freezing protocols to determine the effects of temperature, cooling rate and complete *vs.* incomplete thawing of the ice-ball as these factors may decrease treatment time and complications.

Cryosurgery often does not result in complete cell kill. A more scientific approach to cryosurgery is necessary to better understand the responses of tumour cells to freezing. This will help standardize methods and make tumour cell kill highly reproducible, which in turn will be clinically relevant when applied to improving treatment planning of cryosurgical procedures.

1.6 References

1. Arnott, J. On the treatment of cancers by regular application of an anaesthetic temperature. London, J Churchill (1851).
2. Wroblewski, S.U. and Olszewski, S.K. Liquid state oxygen and nitrogen. *Annalen de Physik* **20**, 256-260 (1883).
3. Dewar, L. Collected papers of Sir James Dewar. Cambridge, Cambridge University Press (1927).
4. White, A.C. Liquid air in medicine and surgery. *Med. Rec.* **56**, 109 (1899).
5. White, A.C. Possibilities of liquid air to the physician. *JAMA* **36**, 426 (1901).
6. White, A.C. Liquid oxygen and x-ray treatment of malignant growths. *Interstate Medical Journal* **9**, 657 (1902).
7. Whitehouse H.H. Liquid air dermatology: It's indications and limitations. *JAMA* **49**, 371 (1907).
8. Cooper, I.S. and Hirose, T. Application of cryogenic surgery to resection of parenchymal organs. *N. Engl. J. Med.* **274**, 15 (1966).
9. Graham, G.F. Cryosurgery. *Clinics in Plastic Surgery* **20**, 131-146 (1993).
10. Dawber, R. Cold kills! *Clinical and Experimental Dermatology* **13**:3, 137-150 (1988).
11. Zhou, X., Tang, Z. and Yu, Y. Ablative approach for primary liver cancer: Shanghai experience. *Surg. Oncol. Clin. N. Amer.* **5**:2, 379-390 (1996).

12. Chuang, C., Chu, C., Chiang, H. and Chou, C. Application of cryoablation in the management of prostate cancer. *Chang Gung Med. J.* **20**, 201-206 (1997).

13. Onik, G. Prostate cryoablation: A reappraisal. *In* "Percutaneous Prostate Cryoablation" (G. Onik, B. Rubinsky, G. Watson and R. Ablin, Eds.), pp. 1-12, Quality Medical Publishing, St. Louis, 1995.

14. Morris, D. Hepatic cryotherapy for cancer: A review and critique. *HPB Surgery*. **9**:2, 118-120 (1996).

15. Ravikumar, T. Interstitial therapies for liver tumors. *Surg. Oncol. Clin. N. Amer.* **5**:2, 365-377 (1996).

16. Wong, W., Chinn, D., Chinn, M., Chinn, J., Tom, W. and Tom, W. Cryosurgery as a treatment for prostate carcinoma: results and complications. *Cancer* **79**:5, 963-974 (1997).

17. Lee, F., Mahvi, D., Chosy, S., Onik, G., Wong, W., Littrup, P. and Scanlan, K. Hepatic cryosurgery with intraoperative US guidance. *Radiology* **202**, 624-632 (1997).

18. Mazur, P. The role of intracellular freezing in the death of cells cooled at supraoptimal rates. *Cryobiology* **14**, 251-272 (1977).

19. Mazur, P. Freezing of living cells: mechanisms and implications. *Am. J. Physiol.* **247**, 125-142 (1984).

20. Mazur, P., Leibo, S. and Chu, E. A two-factor hypothesis of freezing injury. *Exptl. Cell Res.* **71**, 345-355 (1972).

21. Meryman, H. Freezing injury and its prevention in living cells. *Annu. Rev. Biophys.* **3**, 341-363 (1974).

22. Steponkus, P. and Wiest, S. Plasma membrane alterations following cold acclimation and freezing. *In* "Plant cold hardiness and freezing stress: Mechanisms and Crop Implications" (P. Li and A. Sakai, Eds.), pp. 75-91, Academic Press, New York, 1978.

23. Mazur, P. The role of cell membranes in the freezing of yeast and other single cells. *Ann. N.Y. Acad. Sci.* **125**, 658-676 (1965).

24. Levitt, J. and Scarth, G. Frost hardening studies with living cells. II. Permeability in relation to frost resistance and the seasonal cycle. *Can. J. Res. Sect. C. Bot. Sci.* **14**, 285-305 (1936).

25. Steponkus, P., Stout, D., Wolfe, J. and Lovelace, R. Freeze-induced electrical transients and cryoinjury. *Cryo Lett.* **5**, 343-348 (1984).

26. Toner, M., Cravahlo, E. and Karel, M. Thermodynamics and kinetics of intracellular ice formation during freezing of biological cells. *J. Appl. Phys.* **67**, 1582-1593 (1990).

27. Muldrew, K. and McGann, L. Mechanisms of intracellular ice formation. *Biophys. J.* **57**, 525-532 (1990).

28. Steponkus, P. and Dowgert, M. Gas bubble formation during intracellular ice formation. *Cryo-Lett.* **2**, 42-47 (1981).

29. Farrant, J. and Morris, G. Thermal shock and dilution shock as the causes of freezing injury. *Cryobiology* **10**, 134-140 (1971).

30. Karlsson, J. and Toner, M. Long-term storage of tissues by cryopreservation: critical issues. *Biomaterials* **17**:3, 243-256 (1996).

31. Rubinsky, B., Lee, C. and Bastacky, J. The mechanism of freezing in biological tissue: the liver. *Cryo-Lett.* **8**, 370-381 (1987).

32. Rubinsky, B., Lee, C., Bastacky, J. and Onik, G. The process of freezing and the mechanism of damage during hepatic cryosurgery. *Cryobiology* **27**, 85-97 (1990).

33. Whittaker, D. Mechanisms of tissue destruction following cryosurgery. *Annals of the Royal College of Surgeons of England* **66**, 313-318 (1984).

34. Rubinsky, B. The freezing process and mechanism of tissue damage. *In* "Percutaneous Prostate Cryoablation" (G. Onik, B. Rubinsky, G. Watson and R. Ablin, Eds.), pp. 49-68, Quality Medical Publishing, St. Louis, 1995.

35. Whittaker, D. Ice crystals formed in tissue during cryosurgery. *Cryobiology*. **11**, 202-217 (1974).

36. Onik, G., Lee, F. and Bahn, D. Cryosurgical techniques, caveats, and refinements. *In* "Percutaneous Prostate Cryoablation" (G. Onik, B. Rubinsky, G. Watson and R. Ablin, Eds.), pp. 85-128, Quality Medical Publishing, St. Louis, 1995.

37. Sklar, G., Koschorke, G., Filderman, P., Naslund, M. and Jacobs, S. Laparoscopic monitoring of cryosurgical ablation of the prostate. *Surg. Lap. Endo.* **5**:5, 376-381 (1995).

38. Lee, F., Bahn, D., McHugh, T., Onik, G. and Lee Jr., F. US-guided percutaneous cryoablation of prostate cancer. *Radiology* **192**, 769-776 (1994).

39. BioSource International. AlamarBlue™ Assay Product Information Sheet. 1997.

40. Yang, H., Acker, J., Chen, A. and McGann, L. *In situ* assessment of cell viability. *Cell Transplantation* **7**:5, 443-451 (1998).

CHAPTER 2: DEVELOPMENT OF A CRYOSURGICAL MODEL SYSTEM

2.1 Introduction

Cryosurgery is used with increasing frequency in the treatment liver and prostate cancers. The majority of cryosurgical treatment modalities are considered experimental because not enough long-term studies have been performed. In some cases cryotherapy is thought to be as effective as other forms of treatment, although recurrence of disease after therapy is still problematic (1,2,3,4). It is often assumed that the radius of freeze is also the radius of kill within the ice-ball (5). This is presumed since there is a clear demarcation between the frozen and unfrozen sections of the tissue after thaw, which is interpreted as healthy or dead tissue. Cancer recurrence could mean that either the entire tumour was not frozen or some cancer cells survive the freezing process. Therefore, current cryosurgical procedures are inadequate and vital information about tumour cell responses to freezing is lacking.

The current limitations to cryosurgery point to the need for a better understanding of cell and tissue responses to freezing and dynamics occurring within the ice-ball if cryosurgery is to become a reliable alternative to current cancer regimens. A more scientific approach to cryosurgery is necessary to standardize methods and make tumour cell kill reproducible. This is clinically relevant when applied to improving treatment planning of cryosurgical procedures.

Rationale

To help understand what happens to tumours in response to the freezing protocols used in cryosurgery, one must first question what happens to the individual cells within the tissue at various distances from the cryosurgical probe. Basic information is required about the thermal histories and how they relate to outcome in order to develop optimal cryosurgical treatment protocols. These protocols will be experimentally determined and applicable to cryosurgery. In order to realize these goals, we need to develop ways to study the responses of tumour cells in a controlled manner. The purpose of this chapter is to delineate the rationale, objectives, and design of a complete and novel cryosurgical model system that will allow the controlled study of different cryosurgical protocols.

Objectives

The objective of these studies is to describe the development of an experimental model system to allow physical and thermal measurements to be correlated with biological outcomes, in a manner conducive to treatment planning. In order to accomplish this, it was necessary to build a realistic cryosurgical model system, determine adequate biological assessment techniques, and be able to perform and analyze freeze-thaw experiments.

The specific design objectives include: the system must be a physically realistic model of cryosurgery with well defined boundary conditions; it must allow assessment of cryosurgical procedures in a controlled environment to define more effective freeze-thaw protocols; it must be amenable to theoretical descriptions that correlate with experimental measurements in a reproducible

manner to validate the model system and for future theoretical modeling of thermal and cryobiological responses; and it must allow correlation of thermal profiles and freezing conditions with biological outcomes that can be directly applied to improving treatment planning of cryosurgery. The system validation is incorporated into appendix A in this thesis was provided by Mr. Rod Gonzales and Dr. Rick Batycky of the Chemical Engineering Department who mathematically validated the system.

The building of a physically realistic cryosurgical model system requires meeting certain biological objectives including; determination of suitable cells, an appropriate tissue alternative, and adequate biological assessment techniques.

2.2 Materials

Cryosurgical Model System Design

The following description of the cryosurgical model system is presented in figures 2.1, 2.2, and 2.3. The system consists of a disk shaped chamber in which the outer circumference and bottom are made out of Teflon™. The lid is comprised of Plexiglas™ with small holes drilled through the top outward in the radial direction, slightly skewed from one another. The holes on opposite sides of the lid are located equidistant from one another so that point temperature measurements are at the same location as the samples removed from the chamber. The holes on one side will be used to biopsy biological samples from within the chamber and are large enough to accommodate 19 gauge 1½ inch (3.81 cm) needles (Becton Dickinson and Company, Franklin Lakes, NJ). The holes that are located equidistant apart on the opposite side of the lid contain

0.01 inch (0.25 mm) T-type Teflon insulated thermocouples (OMEGA Engineering, Stamford, CT) that are used to measure temperature profiles at specific locations within the sample. Data from the thermocouples is recorded by the DaqBook™ multichannel data acquisition system with DBK 19 thermocouple card (OMEGA Engineering) connected to a computer. There are nine thermocouples penetrating the holes into the chamber that measure temperatures according to radius from the probe. One thermocouple is placed inside the probe to monitor probe interior temperatures at the level of ice-ball formation. For comparison, the probes actual temperature is measured by a thermocouple placed on the exterior of the probe just as it exits the chamber.

A thin stainless steel ring was constructed to fit along the outer circumference of the inner chamber. Attached to the ring are two 4 inch (10.2 cm) tape heaters (OMEGA Engineering) which are used to heat the stainless steel ring and maintain the circumference of the chamber at 37°C. A thermocouple attached to the stainless steel ring monitors the temperature and relays this information to a Micromega CN77000 series controller (OMEGA Engineering) that is responsible for maintaining the outside temperature of the chamber at 37°C.

A stainless steel pipe of outer diameter 4.7 mm and thickness 0.75 mm functions as a cryoprobe and runs axially through the chamber. Stainless steel was chosen because of its relatively high thermal conductivity, capacity to avoid corrosion, and cost effectiveness. The probe is connected at both ends with plastic insulated tubing that act as a conduit for the liquid nitrogen inlet and

outlet. A pressurized Dewar functions as a reservoir and source of liquid nitrogen, and excess liquid nitrogen is collected in an unpressurized collection Dewar.

In these experiments, the experimental chamber contains distilled water, 1X phosphate buffered saline (PBS, GIBCO Laboratories, Grand Island, NY), bactoagar (Difco Laboratories, Detroit, MI), low temperature geling agar (Sigma Chemical Company, Mississauga, ON), gelatin (Knox, Toronto, ON), or methylcellulose (methocel, Sigma Chemical Company). Liquid nitrogen or air flowing through the probe respectively cool or warm the contents of the chamber during experiments.

Cell Culture

The cell lines used in these experiments are PC3 and LNCaP, donated by Dr. Joan Turner of the Cross Cancer Institute. Both are human carcinoma cell lines derived from metastatic prostatic adenocarcinomas (6,7). These cultures proliferate well *in vitro* in a 95% air and 5% CO_2 atmosphere at 37°C. Both cell lines will be compared for suitability in the experiments. The cell line PC3 is grown in F-12K nutrient mixture supplemented with 7% v/v fetal bovine serum (FBS) and 1 mg/L penicillin-streptomycin. The LNCaP cells are cultured in D-MEM/F12 tissue culture media supplemented with 5% v/v FBS and 1 mg/L penicillin-streptomycin (all tissue culture supplies from GIBCO Laboratories, Grand Island, NY). Cell counts were done using a Coulter ZB1 electronic particle counter (Coulter Electronics, Hialeah, FL).

Experimental Medium

The experimental medium is the suspension medium in which the cells are frozen and its main function is to immobilize cells and mimic tissue structure. The medium's secondary function is the prevention of convection within the sample. The gels investigated in these experiments include gelatin (Knox, Toronto, ON), Bactoagar (Difco Laboratories, Detroit, MI), low geling temperature agar (Sigma Chemical Company, Mississauga, ON), and methocel (Sigma Chemical Company). The gelatin is made according to manufacturer's instructions and frozen in the cryosurgical system.

The bactoagar and low geling temperature agar are mixed in concentrations ranging from 0.6% to 0.1% w/w, which are evaluated qualitatively on the basis of rigidity or strength and workability. As a result of the evaluations at different concentrations, freezing experiments are performed on these gels at 0.3% concentration to determine reactions to freezing in the model system.

Methocel has been used for years in many diverse fields including medicine, foods, and cosmetics (8). This substance is a carbohydrate polymer that consists of glucose molecules in long chains with replacement of hydrogen in the hydroxyl groups by methoxy side chains (8,9). Methocel is commonly used as a matrix to culture normal and neoplastic cells (10,11,12,13,14). Typical growth patterns result in colony formation over a prolonged period of time. Methocel (methocel) is prepared according to established lab protocols but at altered concentrations. 1%, 2% and 3% w/w solutions of methocel are made by mixing autoclaved methocel with sterile filtered water at 80-90°C in a biosafety

cabinet. The mixture is stirred and heated for about 30 minutes until all methocel dissolves into solution. The mixture is then removed from heat and stirred for 3 hours until it reaches room temperature, where upon an equal volume of ice-cold sterile 2X PBS is added. The mixture is then stirred in a cold room overnight until the solution clarifies. The mixture is stored in a –20°C freezer and thawed when needed.

Assessment of Membrane Integrity

Syto/ethidium bromide (EB) is a dual fluorescent staining method that allows quantitative assessment of cell plasma membrane integrity and will be examined for compatibility with the system. These dyes emit red or green fluorescence upon exposure to ultraviolet light. Syto (Molecular Probes, Eugene, OR) is a permeable stain that labels all cells by binding to DNA and RNA within cells and is detected by green fluorescence (15). In contrast EB (SIGMA Chemical Company, Mississauga, ON) is a non-permeable dye that only enters cells with damaged plasma membranes. It binds to nuclear DNA, and is detected by red fluorescence (16). Although those cells without intact membranes are actually stained by both dyes, the red of the EB stain is much more pronounced than the green of the Syto, so those cells without intact membranes appear red. EB is provided as a 25 μM stock solution in PBS that is stored at 4°C. Syto is provided as a 12.5 μM stock solution in PBS and stored at –20°C. A working solution of Syto/EB is comprised of 100 μl of EB working solution (15 μl stock EB into 985 μl PBS) with 1000 μl Syto working solution (15 μl Syto stock solution into 985 μl cell culture media).

Metabolic Assay

AlamarBlue™ (BioSource International, Camarillo, CA) is a new metabolic assay that will be investigated and evaluated for assessment of metabolic function of cells after freezing. AlamarBlue functions according to the cell's ability to reduce the dye from its oxidized blue form to reduced pink form and thus indirectly measure cell viability (17). This dye incorporates a REDOX indicator that changes colour in response to chemical reduction of the growth medium as a result of metabolism when it is reduced by cytochromes, $FMNH_2$, $FADH_2$, NADH, and NADPH. AlamarBlue comes in a ready to use formulation. In order to use this assay, determinations of the concentration of cells in suspension is necessary, as well as compatibility with the gel, and time of incubation required for the assay.

2.3 Methods

Cryosurgical Model System Function

First a liquid nitrogen Dewar is filled and pressurized, then attached to the system as shown in figure 2.1. If the particular experiment involves the use of water or 1X PBS, a 30 ml sample is warmed in a 37°C water bath and added to the model system when the sample reaches 37°C. If the experiment uses methocel, a 50 ml sample is warmed in a water bath until the sample reaches equilibrium. Then an 18 gauge needle is attached to a 20 ml syringe and 30 ml of the methocel is removed and added to the model system. The heater is turned on just prior to the addition of media and maintains the outer temperature at 37°C. The lid with thermocouples is secured to the top of the system as soon as

the media is added. Making sure that all the connections in the system are attached, the data acquisition system and liquid nitrogen source are activated simultaneously, marking the beginning of the freezing cycle. The duration of the freezing cycle is 10 minutes (about the average duration of an actual cryosurgical freeze), during which the temperature is recorded at a rate of 1 measurement per second. Upon completion of the freezing cycle, the liquid nitrogen flow is arrested and room temperature air is pumped through the system to slowly warm it back up from freezing. The data is imported into Excel®, temperature profiles are viewed, and then analyzed. The ice-ball radius is determined from the freezing point of the solution out of the recorded data.

Determination of Optimal Media and Membrane Integrity

The three types of gel and methocel were frozen in the model system as described in the previous section. The properties of the media are qualitatively and quantitatively described. The gels are investigated based on their reaction to freezing, toxicity to cells (which is based on Syto/EB test results), the ability of the media to mimic tissue, and compatibility with the assessment techniques. Since only the methocel is able to maintain its structure after freezing, it is the only one that will be investigated for toxicity, tissue mimicry, and compatibility. It was found that upon mixing and freezing methocel that there is an abundance of gas bubble formation, so it is necessary to degas the gel after the addition of cells and mixing, before experimentation. Information about damage to cells will be obtained from both degassing and the methocel itself at the same time. Upon mixing 6.8 ml of approximately 1.1×10^6 cells/ml of freshly trypsinized cells at

37°C with 23.2 ml of 37°C 2.2% w/w methocel, 500 μl is removed to test the initial reaction of cell membrane integrity. The 500 μl sample is mixed with 100 μl of Syto/EB working solution, added to a hemocytometer (Reichert Scientific Instruments, Buffalo, NY), and counts of red vs. green cells are made using dual ultraviolet and brightfield illumination. Suction is attached to the remaining 29.5 ml of methocel/cell suspension in a 37°C water bath for 1 hour (when all the gas bubbles disappear) to degas the methocel. A 500 μl sample is removed and mixed with 100 μl of Syto/EB working solution and red/green counts are made as above.

In the methocel concentration experiments, methocel, 1X PBS, and tissue culture media are warmed in a 37°C water bath. Freshly trypsinized cells at a concentration of approximately 1.1 x 10^6 cells/ml are added to 37°C methocel to yield final methocel concentrations of 1.2, 1.7, 2.2% w/w all containing the same concentration of cells. Approximately 500 μl of the methocel/cell mixture is then mixed with 100 μl of Syto working solution so that they can be visualized under UV illumination. In another container, 37°C 1X PBS is added to stock methocel to get final concentrations of 1.2, 1.7, and 2.2% w/w methocel without cells. This methocel without cells is added to the bottom 2/3 of a small vial (test tube shaped), approximately 1.2 ml in volume. Then approximately 100 μl of the methocel/cell suspension is added to the top of the methocel. The rest of the tube is then filled to the top with methocel. A schematic of this is presented in figure 2.4. The tubes are then covered with parafilm and the heights of the cells within the tubes are documented using the 10X objective of an Axioskop

microscope (Carl Zeiss Inc. Germany) when the tubes are placed on their sides. The tubes are then incubated for a total of 4 hours with cell heights documented at 2 and 4 hours.

Metabolic Assay

For the alamarBlue assay, determination of cell concentration, compatibility with the methocel and incubation times are necessary. Cell culture media and methocel are warmed to 37°C in a water bath. A 1.7% w/w final concentration of methocel is made by mixing 770 µl of stock methocel with 330 µl of cell culture media either with or without cells. Five different concentrations of cells in methocel are made. A 96 well plate is then filled with 3 replicates of each test substance. The contents of the separate 100 µl wells are as follows; 1) media, 2) 1.7% methocel (made with 1X PBS), 3) 1.7% methocel (made with cell culture media) and alamarBlue, 4-8) 5 different concentrations of cells mixed with methocel and alamarBlue, and 9) 1.7% methocel (made with cell culture media). The plate is then incubated for 3 hours at 37°C. The absorbances are read at 1.5, 2.5, and 3.5 hours using a UV Max microplate reader (Molecular Devices Corporation, Menlo Park, CA) with 570 and 600 nm filters. The percent of alamarBlue reduced is calculated using a formula provided by the manufacturer (presented in appendix B) to compensate for the overlapping spectra at 570 and 600 nm (17).

2.4 Results

Cryosurgical Model System Function

Ice does not form immediately upon initiation of liquid nitrogen flow. After a certain period of time, which is usually 30-60 seconds, ice is nucleated on the surface of the probe and progresses outward in a radial direction. Progression of the ice front in the radial direction occurs until the liquid nitrogen source is removed, although near the end of the freezing cycle, the rate of ice growth slows dramatically. In most cases rings of differing shades of white-gray form within the ice-ball. For example, darker gray rings form within the middle of the ice-ball. In some cases small cracks form within the ice-ball, usually within the first half of the ice-ball closest to the probe. By termination of freeze, the ice-ball covers roughly ¾ of the chamber's radius, but does not reach the edge that is maintained at 37°C.

Examples of typical temperature profiles for the freezing of water, 1X PBS, and 1.7% methocel are represented in figures 2.5, 2.6, and 2.7. In most cases the probes interior temperature reaches liquid nitrogen temperatures (-196°C) by 30 seconds into the freeze and the probes exterior temperature reaches -196°C within the first minute. Once the temperature of the probe cools it remains at a constant temperature of -196°C for the duration of the experiment, until warmed using room temperature air. The heater temperature that maintains the periphery of the model system at 37°C, never goes below 36°C throughout the entire freeze. Most evident in these temperature profiles is the dramatic temperature gradient in the probe and the first few millimeters of media. This steep gradient is

present for approximately the first 6.5 mm radially outwards from the probe. These are the locations of the fastest rates of cooling that will be seen throughout the freezing process. The cooling rates are similar for most freezes, with the highest cooling rates averaging about 220°C/minute at the probe itself. The cooling rates and end-point temperatures are fastest and coldest closest to the probe and get progressively slower and warmer with increasing distance from the probe. The rate of ice-ball growth is fastest in the methocel, slightly slower in water, and slowest in PBS. Figure 2.8 contains ice-ball growth information with respect to time.

Each temperature profile is characteristic of the particular medium being frozen. For example, the choppy nature of the water freeze profile is characteristic of all the water freeze profiles. The dip in the PBS freeze profile as seen in the channel 4 curve is characteristic of all the PBS freezes. Although one might see a bit of a dip in the methocel profile in channel 4, it is generally much smoother. The methocel freeze final temperatures are slightly lower than either of the water and PBS freezes.

Cell Line Choice

From a physical standpoint, cell line choice is based on cell growth, the ease in which the cell line can be manipulated, and how it reacts to these manipulations. For example, how the cells react to trypsinization, mixing, and degassing of the methocel impacts their use in experiments. PC3 cells reach confluency about twice as fast as the LNCaP cells and with a higher cell density at confluency. Upon trypsinization, the PC3 cell line easily form single cells in

suspension, even at concentrations well above $1x10^6$ cells/ml. The LNCaP cells tend to form clumps upon trypsinization, even at low cell concentrations. At the higher concentrations required for experimentation, the formation of clumps is inevitable and breaking apart these clumps results in increased damage to cells.

Optimal Freezing Medium and Syto/EB

The media's reaction to freezing is one of the major contributing factors to selection. All of the gels looked the same when frozen, and seem adequate until thaw. At this point, the agars and gelatin fail to maintain their viscosity, and liquefy. The methocel forms many gas bubbles when frozen, although it maintains all of its physical properties after thawing. The maintenance of methocel properties along with the ability to degas the media, which eliminates bubble formation, is the reason it was chosen. Methocel's lack of toxicity and ability to mock tissue by suspension of cells is further examined.

The viscosity of methocel increases with increasing concentration, but also becomes very hard to work with as the concentration increases. It is important to know at what minimum concentration the methocel is no longer capable of suspending the cells. A table of the distance traveled in 4 hours *vs.* concentration is presented in table 2.1. It is quite evident that the 1.2% solution is incapable of suspending cells for any length of time. A comparison of the 1.2% methocel solution to the 1.5, 1.7, and 2.2% solutions shows a statistically significant difference ($p<0.05$) when using the Student-Newman-Keuls and Tukey tests for pairwise multiple comparison. There are no significant differences

between the 1.5, 1.7, and 2.2% solutions of methocel. Therefore, the 1.7% is chosen since it is slightly more viscous but still easy to work with.

When cells in suspension are mixed with methocel, large numbers of bubbles are formed in solution so it becomes necessary to degas the gel to remove bubbles. The results of the degassing experiments using Syto/EB are examined next. The appearance of cells stained with Syto/EB is usually documented in tissue culture media, where membrane intact cells appear green and non-intact cells appear red. The appearance of the cells in methocel is the same as those in tissue culture media, except that the concentration of Syto/EB necessary is higher in methocel in order to maintain the brightness and colour of the dye. When using the lower concentrations of dye, the Syto may appear very faint green in colour and the EB appears more orange-green than red.

Table 2.2 summarizes the effects of degassing by looking at the percentage of cells with intact membranes. The average of membrane intact cells after degassing and non-degassing is 99% with a standard error of 1.25 and 1.5 respectively. Kruskal-Wallis one way analysis of variance finds that there is no statistically significant difference between the groups ($p=0.677$).

Metabolic Assay

AlamarBlue is a dark blue dye in its non-reacted oxidized form. When alamarBlue is added to methocel, it remains blue and no change in absorbance is seen in the control wells without cells over the entire incubation. The initial blue colour slowly changes into purple, then pink in its reduced form. In the wells containing alamarBlue and cells in methocel, the solution becomes increasingly

pink with time and larger numbers of cells. When the samples that have completely reacted are incubated for long periods of time (in excess of 24 hours), the pink colour slowly subsides and the media will turn colourless. The wells containing tissue culture media and methocel with alamarBlue showed no changes in colour or absorbance. A graph of alamarBlue reduced versus cell number at 2.5 hours is presented in figure 2.9. The experimental data points are best fit to a logarithmic equation as demonstrated by the curve in the graph.

2.5 Discussion

The purpose of these studies is the development and design of a complete and novel cryosurgical model system that will allow the controlled study of different cryosurgical protocols. These efforts tie together both the biological and physical aspects of cryosurgery. The biological aspects in this case refer to the cells, suspension medium, assessment techniques, and cellular responses as a result of defined temperatures, cooling rates and protocols. The physical aspects refer to the system, including both its design as well as function and includes temperature, rates of cooling, and ice-ball size and geometry.

Cryosurgical Model System

Many other cryosurgical model systems have been designed for different purposes. The main reasons for developing these systems include modeling of ice formation (18), evaluation of cryosurgical device function (19,20,21,22), mathematical modeling of temperature distributions in frozen tissue and ice-ball size (23,24), and determination of cellular and tissue destruction with respect to thermal history (25,26,27). The techniques and systems used vary from model to

model based on suitability for the particular types of experiments performed. The choices made for this particular model system are based on specific design objectives, the first of which includes the system being a physically realistic model of cryosurgery with well defined boundary conditions. One of the similarities to *in vivo* cryosurgery is the maintenance of physiological temperatures at the edges of a cryolesion. Although the temperature at the periphery of the experimental chamber decreases to 36°C during the procedure, this is equivalent to the mild whole body hypothermia experienced by patients during cryosurgery. The above mentioned cryosurgical models maintain different constant temperatures at the boundary that range from just above freezing to actual physiological temperatures.

Also similar to real cryosurgical procedures, is the maintenance of probe temperatures once the probe has cooled down. This is seen in all of the temperature profiles in this chapter and is consistent with previous reports on *in vivo* and *in vitro* cryosurgery regardless of the type of media or tissue frozen (19,20,25,27). Therefore, one would expect that cells in the media within the chamber would undergo similar temperature profiles and freezing processes and be analogous to *in vivo* cryosurgery.

The material of choice for the chamber was based upon the low thermal conductivity, insulating capacity, and availability of Teflon™, which can be shaped into the desired form and is biologically inert. Both the air space and lid serve to insulate the chamber and minimize heat loss. The choice of material for the lid was not only based on its insulating properties, but also on the fact that it

is clear and allows visualization of the freezing process. Based on the insulating properties of the materials, an assumption is made that the chamber is completely insulated and that the only heat transfer that occurs is at the probe surface.

It is important to note that the experimental chamber is not designed to simulate the effects of blood vessel damage. Many researchers have reported that cell death is much higher *in vivo* than *in vitro* and is postulated to occur from ischemia after thawing as a result of blood vessel damage (28,29). The overall damage is a combination of direct freezing injury as well as ischemia. Therefore, the rates of cell kill in this thesis reflect only direct freezing injury and are the minimum expected injuries in cryosurgery.

The controlled manner in which the system is frozen and protocols maintained are other design objectives. The temperature controller and data acquisition system along with all of the thermocouples allow real time monitoring of the freezing process. The error in thermocouple measurement is approximately ±1.4°C, which may introduce some error in determining exact temperatures (30). The addition of thermocouples themselves interjects errors in temperature measurement due to heat conduction by the thermocouple, which heats the point of measurement (31). Error in thermocouple placement is minimized due to fixation within the lid.

When considering the temperature profiles of all three media, one of the obvious properties is the presence of a delay in cooling between the interior of

the probe and the exterior of the probe. This is because the probe itself must be cooled before cooling of the sample occurs.

All three of the different freezing protocols are very similar to one another including profile shape, cooling rates and final temperatures. There are some minor differences between the graphs, some of which are probably due to the nature of the substance being frozen, and others due to experimental inconsistencies. The only difference that may occur between experiments is in the control of flow rate. The switch that controls liquid nitrogen flow out of the Dewar may not be precise enough to distinguish between two slightly different rates of flow. As a result, one can see that in fact there are slight variations in the cooling rates not only between the three media, but also between the different freezes of the same media. This may also contribute to the differences in ice-ball growth between the three media.

When examining the water freeze, small, sharp dips occur in the freezing profile that are not apparent in the freeze profiles of the other two media. This particular profile looks very similar to water freeze profiles from experiments freezing water by other investigators comparing different probes for function (20). Therefore, this peculiarity is likely associated with the nature of freezing water. It is not suspected that these are changes is liquid nitrogen flow since they only appear in the water freezes. Other than these differences the water freeze highly resembles the methocel freeze.

The 1X PBS freeze profile resembles the methocel profile with respect to its smoothness and shape, but has some differences. For example, the ice-ball

does not grow to be as large as the one in methocel and there is a small indentation in the freezing profile of the first thermocouple in PBS. However, it should be noted that the ice-ball in water does not grow to be as large as the ice-ball in methocel. The fact that water and PBS are capable of convection, unlike the methocel, may be what is responsible for this phenomenon. Since the outside of the chamber is maintained at 37°C, the convection currents could circulate the warmer outer fluid to the edge of the ice-ball, slowing its growth.

The methocel profiles are very similar to tissue freezing profiles seen in other investigator's work when a whole liver is perfused by 37°C water and frozen using a clinical cryoprobe (18). Also, many experiments with gels such as agar and gelatin demonstrate similar freezing properties when compared to tissues (19,20,24,25). Based on the knowledge that the tissue freezing profiles are similar to the methocel profiles and different from the water and PBS profiles, in this thesis we assume that methocel is similar to tissue and is a good choice for tissue comparison. This assures us that the model system is functioning consistently compared to real cryosurgical systems. This cryosurgical system that has been developed meets with the set design objectives. It is a physically realistic model and an excellent choice for performing biological response experiments.

Medium

As mentioned, in other investigated work, different freezing media are being used depending on the type of experiment. In some cases 1, 1.5 or 5% w/w gelatin and 99, 98.5 or 95% water was used as the test medium

(18,19,24,25). A 0.3% agar and 2% agarose (w/w) have also been used in some cases (20). These test media are said to simulate tissue very closely in its freezing properties, however this does not take into consideration the solutes that would normally be present in tissues. Also, although many of these gels have similar freezing properties, they do not maintain their structure after thawing, as real tissue does. In the other investigators experiment, the main purpose of the various suspension media is the prevention of convection within the sample during freezing and no cells are used.

When using cells, they must be suspended in a physiological solution to prevent lysis. Another experiment uses droplets of cells suspended in tissue culture media and freezes them on a directional solidification stage (27). Experiments using small droplets do not take into account the extent of mass transfer and accumulation of solutes in advance of the freezing front that would occur on a larger scale in real tissues. Many experiments freeze actual tissue or organs. Some such experiments freeze a thin slice of tissue on a cryomicroscope or directional solidification stage and then test tissue viability (27). One problem with organs and tissues is the difficulty in looking at individual cells within the tissue and assessing damage.

Another difference between methocel and the gels is that methocel forms bubbles upon mixing. This is easily avoided by degassing the methocel before adding it to the system. The experimental evidence shows that there is no significant difference between the membrane integrity of the degassed and non-degassed cells, therefore degassing can occur without any damage to the cells

within the methocel. Also as a result of the experiments, it has been shown that staining of cells using Syto/EB allows almost effortless visualization of cells using dual brightfield and UV illumination. The presence of the methocel does not interfere with the assay.

The water, PBS, and the methocel all form bubbles upon freezing, since it is a normal part of the freezing process. During the freezing process, gaseous solutes are concentrated in advance of the freezing front and will form a concentration gradient as dissolved salts do (32). At some point, nucleation of gas bubbles occurs. The bubbles continue to grow and may precipitate out of solution and become encapsulated within the ice. When gas bubbles are encapsulated the concentration gradient can build up again.

When methocel is frozen in the cryosurgical model system, the appearance of ice formed around the probe looks similar to the ice formation described around an actual cryosurgical probe in both salt solution and gelatin (18). When the ice is broken apart and examined, it consistently breaks apart in the same manner, parallel to the radial direction of ice growth. The edges of the frozen methocel resemble the elongated ice crystals growing in the radial direction. Therefore the spicular ice formation behavior of methocel is consistent with other media used to freeze cells and the same as ice formation that is thought to occur in tissues.

It is important to note that methocel is not actually a gel, but rather a very viscous solution. It reacts much more like tissues would to freezing, by maintaining its shape and consistency. The advantage of using methocel over

real tissues is the ease in which samples can be biopsied and used in viability assessments. Also, studying the effects of freezing injury is difficult in tissues since they are so closely packed and are influenced by the presence of blood vessels. Therefore methocel is a model representative of a tissue system that allows the study of an intermediate step between that of real tissues and single cells in suspension that has not been available previously.

Assessment Techniques

The assessment of alamarBlue in this chapter is limited to determining the numbers of cells required for analysis, the time of incubation, and compatibility with the methocel. The incubation times in methocel are similar to the manufacturer's recommendations for alamarBlue in media (3-4 hours) (17). When methocel and alamarBlue are combined, there is no change in absorbance. Therefore alamarBlue is non-reactive with the methocel and is appropriate for use as an assessment technique for the cryosurgical model system.

Syto/EB is a simple, quick, and reliable method to determine cell plasma membrane integrity, but there are questions concerning the relationship between membrane integrity and cell death. If cells without intact membranes are capable of repair, staining by EB is only an indicator of cell injury rather than death. Ethidium bromide does not give information about cell function, therefore alamarBlue can be used as an alternative to compare results. Comparisons of Syto/EB results to alamarBlue will be a component of the following chapters when freezing of the biological components occurs.

This new cryosurgical model system is a physically realistic model of cryosurgery that allows assessment of cryosurgical procedures in a controlled environment. It is amenable to theoretical descriptions that correlate with experimental measurements. The goal achieved with this work is the development of an experimental model system that allows physical and thermal measurements to be correlated with biological outcomes. This was accomplished by designing a realistic cryosurgical model system, validating biological assessment techniques, and performing and analyzing freeze-thaw experiments. This model system will be used in the following chapters, after incorporating cells, to determine more effective freeze-thaw protocols that could be used in improving cryosurgery in a manner conducive to treatment planning.

2.6 References

1. Chuang, C., Chu, C., Chiang, H. and Chou, C. Application of cryoablation in the management of prostate cancer. *Chang Gung Med. J.* **20**, 201-206 (1997).
2. Morris, D. Hepatic cryotherapy for cancer: A review and critique. *HPB Surgery* **9**:2, 118-120 (1996).
3. Ravikumar, T. Interstitial therapies for liver tumors. *Surg. Oncol. Clin. N. Amer.* **5**:2, 365-377 (1996).
4. Wong, W., Chinn, D., Chinn, M., Chinn, J., Tom, W. and Tom, W. Cryosurgery as a treatment for prostate carcinoma: results and complications. *Cancer* **79**:5, 963-974 (1997).
5. Rubinsky, B. The freezing process and mechanism of tissue damage. *In* "Percutaneous Prostate Cryoablation" (G. Onik, B. Rubinsky, G. Watson and R. Ablin, Eds.), pp. 49-68, Quality Medical Publishing, St. Louis, 1995.
6. Kaighn, M., Shankar Narayan, K., Ohnuki, Y., Lechner, J., and Jones, L. Establishment and characterization of a human prostatic carcinoma cell line (PC3). *Invest. Urol.* **17**:1, 16-23 (1979).
7. Horoszewicz, J., Leong, S., Kawinski, E., Karr, J., Rosenthal, H., Chu, T., Mirand, E., and Murphy, G. LNCaP model of human prostatic carcinoma. *Cancer Res.* **43**, 1809-1818 (1983).
8. Tomioka, M. and Matsumura, G. Effects of concentration and degree of polymerization on the rheological properties of methylcellulose aqueous solution. *Chem. Pharm. Bull.* **35**:6, 2510-2518 (1987).

9. Liesegang, T. Viscoelastic substances in ophthalmology. *Surv. Ophthalmol.* **34**:4, 268-293 (1990).

10. Kluin-Nelemans, H., Hakvoort, H., Jansen, J., Duinkerken, N., van den Burgh, J., Falkenburg, F., and Willemze, R. Colony growth of normal and neoplastic cells in various concentrations of methylcellulose. *Exp. Hematol.* **16**, 922-928 (1988).

11. Pavlik, E., Kenady, D., Van Nagell, J., Keaton, K., Donaldson, E., Hanson, M., and Flanigan, R. The proliferation of human tumor cell lines in the presence of different agars, agaroses, and methyl cellulose. *In Vitro* **19**:7, 538-550 (1983).

12. Cillo, C., Schreyer, M. Odartchenko, N., and Carrel, S. Histological analysis of human tumour cell colonies grown in methylcellulose cultures. *Br. J. Cancer* **49**, 653-657 (1984).

13. Kanemoto, T., Tohya, K., Kimura, M., Fukuyama, A., and Kitamura, Y. Effects of culture matrix on differentiation of murine mast cells. *Exp. Hematol.* **19**, 288-293 (1991).

14. Bossart, E. and Conti, G. Epidermal growth factor stimulates colony formation and non-neuronal marker protein expression by human neuroblastoma in methylcellulose culture. *Anticancer Res.* **9**, 1497-1504 (1989).

15. Molecular Probes. Syto. Package insert.

16. Edidin, M. A rapid, quantitative fluorescence assay for cell damage by cytotoxic antibodies. *J. Immunol.* **104**, 1303-1306 (1970).

17. BioSource International. AlamarBlue™ assay. Package insert.

18. Kaprelyants, A., Kaprelyants, A., and Migunova, R. Microscopic study of the ice formation process around a cryosurgical probe. *Cryo-Lett.* **19**, 303-308 (1998).

19. Chang, Z., Finkelstein, J., Ma, H., and Baust, J. Development of a high-performance multiprobe cryosurgical device. *Biomed. Inst. Tech.* **28,** 383-390 (1994).

20. Kaplan, S. Greenberg, R., and Baust, J. A comparative assessment of cryosurgical devices: application to prostatic disease. *Urology* **45**:4, 692-699 (1995).

21. Dilley, A., Dy, D., Warlters, A., Copeland, S., Gillies, A., Morris, R., Gibb, D., Cook, T., and Morris, D. Laboratory and animal model evaluation of the Cryotech LCS 2000 in hepatic cryotherapy. *Cryobiology* **30**, 74-85 (1993).

22. Rabin, Y. and Shitzer, A. A new cryosurgical device for controlled freezing: I Setup and validation tests. *Cryobiology* **33**, 82-92 (1996).

23. Poledna, J. and Berger, W. A mathematical model of temperature distribution in frozen tissue. *Gen. Physiol. Biophys.* **15**, 3-15 (1996).

24. Bischof, J., Merry, N., and Hulbert, J. Rectal protection during prostate cryosurgery: design and characterization of an insulating probe. *Cryobiology* **34**, 80-92 (1997).

25. Homasson, J.P., Thiery, J.P., Angebault, M., Ovtracht, L., and Maiwand, O. The operation and efficacy of cryosurgical, nitrous oxide-driven

cryoprobe I Cryprobe physical characteristics: their effects on cell cryodestruction. *Cryobiology* **31**, 290-304 (1994).

26. Rabin, Y., Coleman, R., Mordohovich, D., Ber, R., and Shitzer, A. A new cryosurgical device for controlled freezing II. *In vivo* experiments on skeletal muscle of rabbit hindlimbs. *Cryobiology* **33**, 93-105 (1996).

27. Bischof, J., Smith, D., Pazhayannur, P., Manivel, C., Hulbert, J., and Roberts, K. Cryosurgery of Dunning AT-1 rat prostate tumor: thermal, biophysical, and viability response at the cellular and tissue level. *Cryobiology* **34**, 42-69 (1997).

28. Rubinsky, B., Lee, C. and Bastacky, J. The mechanism of freezing in biological tissue: the liver. *Cryo-Lett.* **8**, 370-381 (1987).

29. Rubinsky, B., Lee, C., Bastacky, J. and Onik, G. The process of freezing and the mechanism of damage during hepatic cryosurgery. *Cryobiology* **27**, 85-97 (1990).

30. OMB-DAQBOOK/DAQBOARD: Data acquisition hardware and software for notebook and desktop PCs users manual, Revision 4.1. Stamford, CT. 1996.

31. Rabin, Y. Uncertainty in temperature measurement during cryosurgery. *Cryo-Lett.* **19**, 213-224 (1998).

32. Korber, C. Phenomena at the advancing ice-liquid interface: solutes, particles and biological cells. *Quarterly Rev. Biophys.* **21**:2, 229-298 (1988).

Figure 2.1 Photograph of the cryosurgical model system.

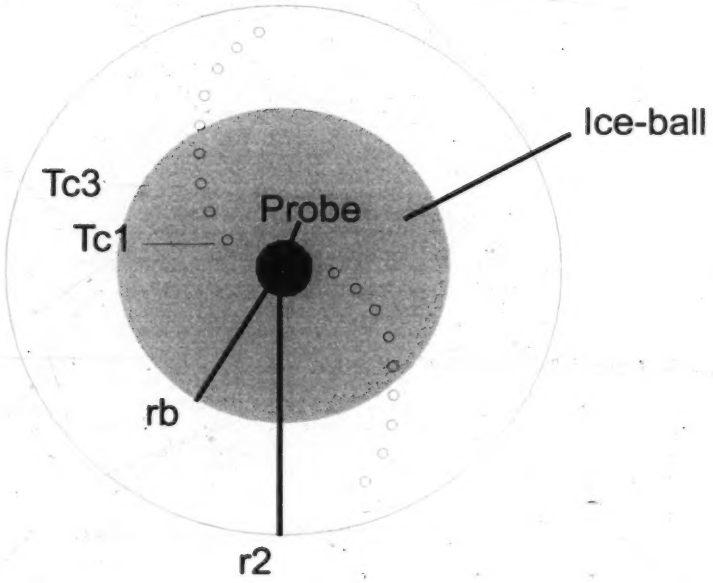

Figure 2.2 Cryosurgical chamber viewed from above. The probe is located centrally within the system. The holes represent thermocouple and biopsy sites. Tc1 and Tc 3 represent the first and third thermocouples in the chamber while rb and r2 are the radii of the ice-ball and chamber respectively.

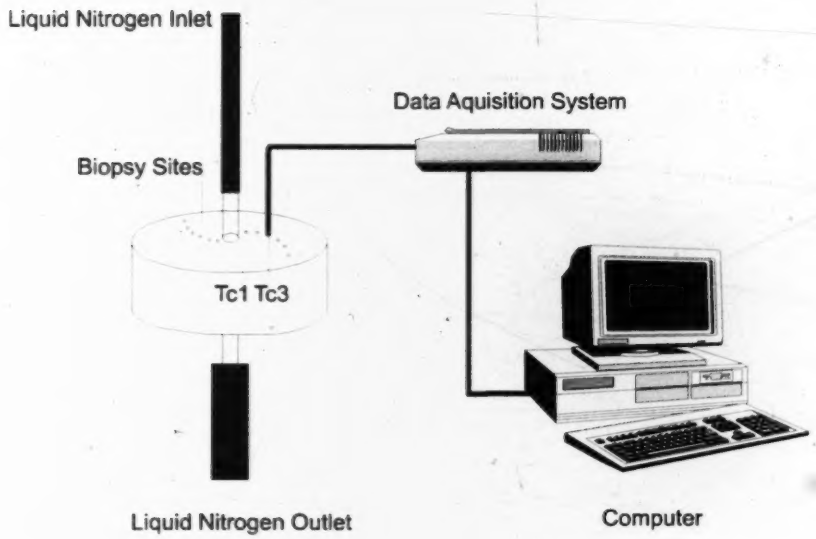

Figure 2.3 Cryosurgical model system set up.

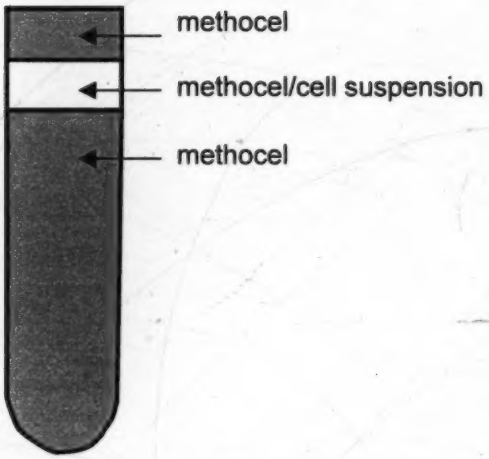

Figure 2.4 Schematic of methocel concentration experiments. A layer of cells in a methocel suspension is sandwiched between two layers of methocel of the same concentration.

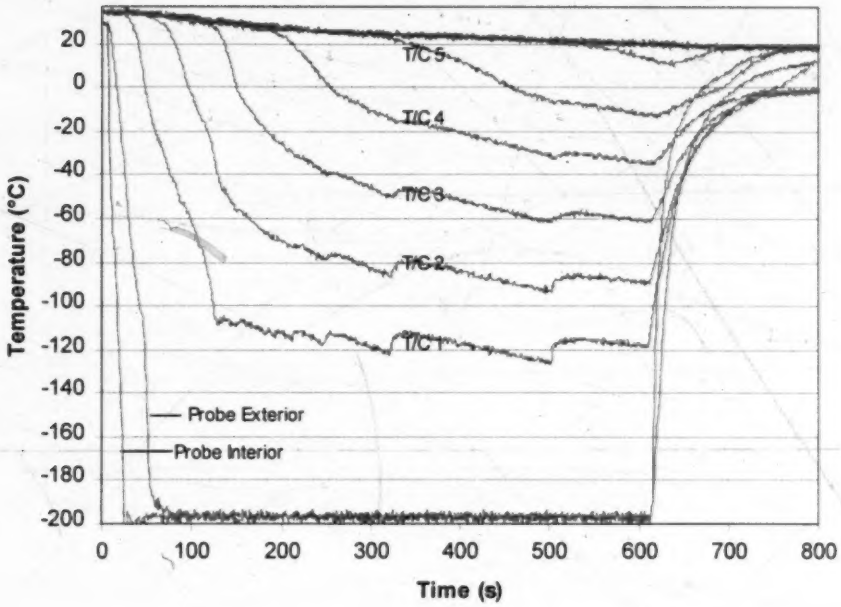

Figure 2.5 Example of water freeze temperature profiles. The first two curves on the bottom of the graph represent the temperatures inside and outside the probe. The curves above the probe temperatures are the freezing profiles of water at increasing distance from the probe.

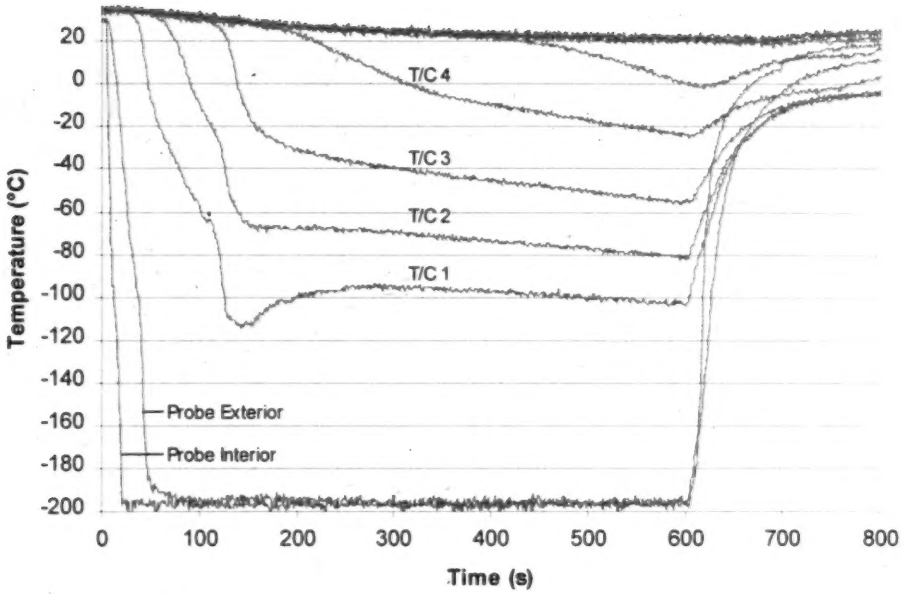

Figure 2.6 Example of PBS freeze temperature profiles. The first two curves on the bottom of the graph represent the temperatures inside and outside the probe. The curves above the probe temperature curves are the freezing profiles of the PBS at increasing distances from the probe.

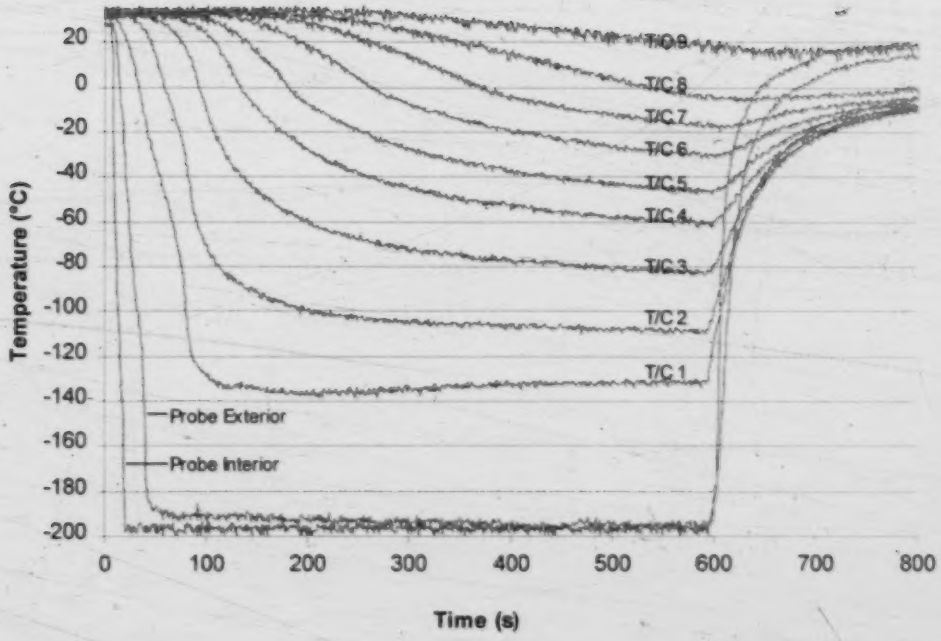

Figure 2.7 Example of methocel freeze temperature profiles. The first two curves on the bottom of the graph represent the temperatures inside and outside the probe. The curves above the probe temperatures are the freezing profiles of the methocel at increasing distance from the probe.

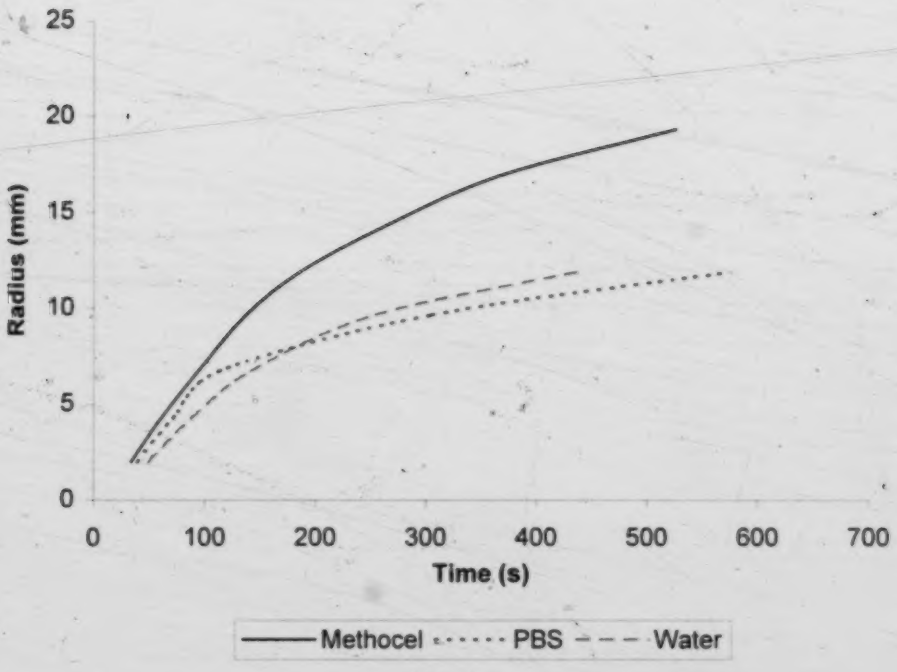

Figure 2.8 Graph of ice-ball growth versus time in methocel, PBS and water. The growth of the ice-ball in methocel is greater than in either one of the other media.

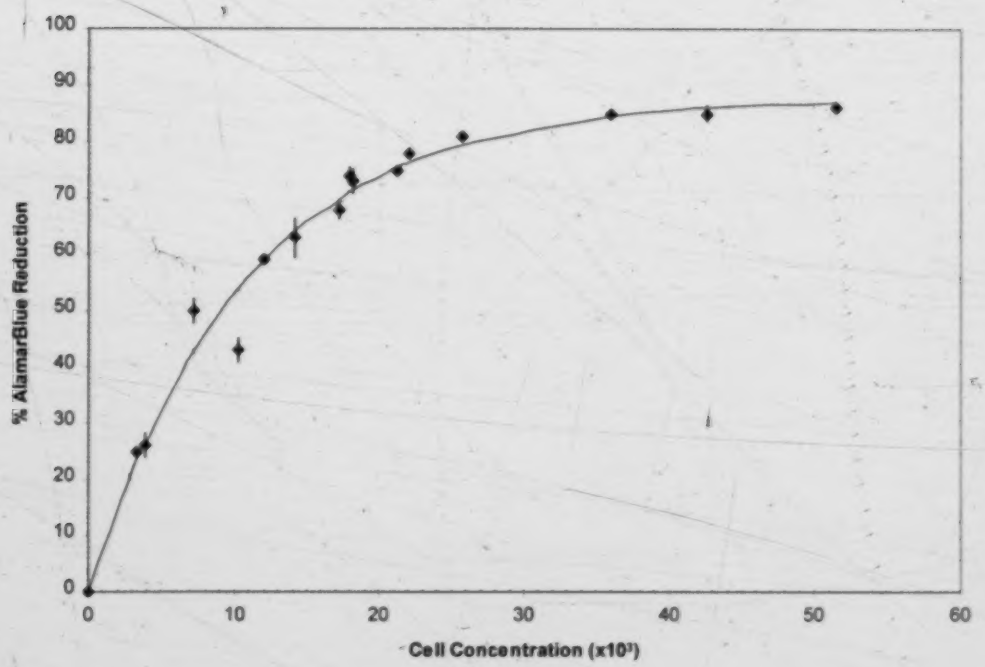

Figure 2.9 Graph of percent alamarBlue reduced versus PC3 cell concentration at 2.5 hours.

Methocel Concentration (% w/w)	Distance Travelled (mm)
1.2	7.4 ± 2.1
1.5	1.2 ± 0.8
1.7	0.3 ± 0.2
2.2	0.2 ± 0.2

Table 2.1 Distance PC3 cells travel within the methocel medium after 4 hours incubation for various methocel concentrations.

Membrane Intact (%)	
Gas	Degassed
99 ± 1	99 ± 1
100 ± 0	98 ± 1
98 ± 2	100 ± 0
100 ± 0	99 ± 1
99 ± 0	99 ± 0

Table 2.2 This table shows the percent of PC3 cells with intact membranes before and after degassing. The data are represent four different samples taken from five separate experiments.

CHAPTER 3: BIOLOGICAL RESPONSES TO SINGLE AND DOUBLE FREEZE

3.1 Introduction

This newly developed cryosurgical model system will now incorporate biological aspects and be used to examine the responses of cancer cells to freezing at low temperatures. This chapter focuses on the relationship between cell viability and cryosurgical conditions during the freezing process. Since the 1960s the basic parameters of a cryosurgical procedure have been firmly incorporated and include rapid freezing, slow thawing, and repeating freeze-thaw cycles. Still, recurrence of disease is problematic in many cases. To make cryosurgery more successful, basic information about the thermal histories and how they relate to outcome is needed. It will become necessary to develop specific optimal protocols that have been experimentally proven to work, are based on sound scientific evidence, and that are applicable to cryosurgery. The first step in this process involves studying the basics of biological outcome under controlled freezing conditions. Understanding the thermal conditions necessary for cancer cell destruction would be very useful. If we were able to establish measurable and predictable biological outcomes as a result of specific freezing protocols, this could then be applied to altering cryosurgical protocols to maximize cellular destruction during cryosurgery.

During cryosurgery the destructive effects that are a result of freezing tissue are due to a wide range of factors. These factors can be divided into two groups based on their ability to cause immediate or latent injury. In the first case, immediate damage refers to direct cell injury as a result of the freezing and

thawing processes (1). Latent injury refers to vascular stasis, where ischemia is the primary cause of injury (2,3). It is important to note that this study does not endeavor to study the effects of vascular stasis as one of the primary causes of tissue death *in vivo*. In fact, one of the problems associated with experiments on cell death *in vivo* is that the effects of vascular stasis obscure damage that occurs as a result of direct cell injury from freezing. This model system allows separation out of the purely cryobiological aspects of direct cell injury from the indirect.

Direct cell injury begins even before cells are frozen. Death can result from hypothermic damage as the temperatures fall below physiological temperatures, but above freezing temperatures (4). The function and structure of cells can be altered adversely, and if held for long enough duration, may lead to death.

The majority of damage that occurs during freezing is a result of ice formation and alterations to water content within tissues. Injury is associated with solution effects, intracellular ice formation and recrystallization upon warming (17). The amount of damage caused by different types of ice formation changes depending on the distance from the cryoprobe and on different properties of the freezing cycle. These properties include cooling rate, end tissue temperature, duration of freeze, rate of thawing, number of freeze-thaw cycles, and the amount of time between freeze-thaw cycles (1,5,6).

Rapid cooling rates in cryosurgery cause more damage than slower cooling rates (5). Rapid cooling rates greater than 50°C/min are present in cryosurgery, but only in the areas closest to the cryosurgical probe (7,8). Intracellular ice formation is associated with these rapid rates of cooling and is considered lethal

(9). At the periphery of the ice-ball, cooling rates are much slower and the probability of intracellular ice formation is much lower. This is one reason why increased numbers of cells at the edge of the ice-ball survive the freezing process.

The end tissue temperature is also of great importance during cancer cryosurgery. An end temperature of less than –50°C is necessary to ensure tumour cell death in many studies (10). This is another reason for cancer cell survival in the periphery of the ice-ball. If cryosurgery is to be used as an alternative to current cancer regimens, lethal tissue temperatures become important.

Prolonging the duration of freeze has been found advantageous by some investigators (5). This is thought to be more important in the periphery of the ice-ball where temperatures are above –50°C. The amounts of damage caused by solution effects increase with time (11), so it is thought that cells at the edge of the ice-ball are allowed to incur more damage. Also, if the amount of time during thawing is increased, prolonging the exposure of cells to temperatures where recrystallization occurs increases the ice crystal size and injury to cells (1,3). Decreasing the thawing rate also decreases cell survival for the same reason, since it allows for recrystallization which is damaging to cells.

In this chapter the biological responses of cancer cells to a single freeze-thaw cycle will be examined at a probe temperature of –196°C, as the first step towards establishing measurable biological outcomes under specific freezing conditions. It will be possible to create a scale of cell kill at a given radius as a function of cooling rate, temperature, duration, and number of cycles.

Although some surgeons and researchers still think that a single freeze-thaw cycle is sufficient to kill tumour cells, it is widely accepted that double freeze-thaw cycles enhance the amount of damage to cells and as a result, this techniques is widely used during cryosurgical procedures (3,12,13,14). The actual amounts of increase in cell kill are not well documented and the effects of repetition vary from one case report to the next. This chapter will examine the effects of a double freeze-thaw protocol on cells. The double freeze-thaw experiments are designed to clarify the extent of the resulting cellular damage and effects of repeat freezing. The effects of a double freeze-thaw cycle are thought to be caused by the fact that cells are subjected to twice the deleterious temperatures that cause damage as well as increasing the time the cells spend at sub-zero temperatures (1).

3.2 Materials and Methods

Cell Culture

Tissue culture is performed as described in chapter 2. In summary, the PC3 cell line is grown in F-12K nutrient mixture supplemented with 7% v/v FBS and 1 mg/L penicillin-streptomycin at 37°C in an atmosphere of 95% air and 5% CO_2. Cells are grown in 75 cm^2 flasks and trypsinized when near confluent using 0.25% trypsin with EDTA (all tissue culture supplies from GIBCO Laboratories, Grand Island, NY). After the cells are detached, they are resuspended in media and counted. The cell concentration is adjusted to approximately 1.1 X 10^6 cells/ml for all experiments.

Media Preparation

The methocel is stored in a –20°C freezer and when needed, is immersed in a water bath until it reaches 37°C. At this point, 9.1 ml of cell suspension at a concentration of 1.1 X 10^6 cells/ml is mixed well into 20.9 ml 37°C methocel. A vacuum is then attached to the cell-methocel suspension while remaining in a 37°C water bath for a period of 1 hour, until all trapped air bubbles are out of the methocel. The heater (OMEGA Engineering, Stamford, CT) that maintains the cryosurgical system periphery at 37°C is turned on, and the cell mixture is added and the experiment begins.

Cryosurgical System and Freezing Protocols

The cryosurgical system is the same as described in chapter 2 of this thesis. Freezing can begin once the cells and medium are added to the system. The liquid nitrogen source and temperature monitoring devices are activated after the lid and supply hoses are secured in place. The single freeze-thaw protocol consists of 10 minutes of continuous freezing. Liquid nitrogen flow is arrested at this point, and the sample is warmed using room temperature air flowing through the supply tube until no ice remains. In the double freeze-thaw protocol, the methocel is once again frozen for a period of 10 minutes. The system is warmed using room temperature air after the second 10 minute freeze, which allows all the methocel and thermocouples to equilibrate to room temperature in approximately 25 minutes.

Samples are removed from the chamber when the interior of the chamber reaches room temperature, using 19 gauge 1½ inch (3.81 cm) needles and a 1

ml syringe inserted through the biopsy sites in the lid. One 200 µl sample is removed from each biopsy site (9 from the system plus 2 controls). The positive control consists of cells in methocel biopsied before freezing, where cell viability is approximately 100%. The negative control consists of a biopsy of cells in methocel that have been subjected to 15 freeze-thaw cycles and all of the cells are dead as verified experimentally by alamarBlue and membrane integrity assays. The samples are incubated for 1 hour at 37°C in 5% CO_2 and used in assays to determine viability.

Syto/EB

The Syto/EB is prepared and used in the same manner as described in chapter 2. Membrane integrity is evaluated 1 hour post-thaw after mixing 100 µl of the cell suspension with 20 µl of Syto/EB and allowing 5 minutes for the dye to penetrate the cells. Cells are counted under dual fluorescent-brightfield illumination using a hemocytometer (Reichert Scientific Instruments, Buffalo, NY) and an Axioskop microscope (Carl Zeiss Inc. Germany). For each experiment, 4 counts are made from each biopsy site.

AlamarBlue

The remaining 100 µl of cell suspension and 10 µl of alamarBlue are added to a 96 well plate (Corning Glass Works, Corning, NY) and incubated at 37°C in a 5% CO_2 incubator for 2.5 hours. The absorbance is read using a UV Max microplate reader (Molecular Devices Corporation, Menlo Park, CA) at 570 and 600 nm. The percent of alamarBlue reduced is calculated using a formula provided by the manufacturer to compensate for the overlapping spectra at 570

and 600 nm (15). The number of viable cells can be found using the standard graph from chapter 2 and the equation derived from this graph. Knowing the percent reduction allows calculation of the number of cells that are alive. The number of dead cells can be deduced from the fraction of cells remaining from the original cell concentration.

3.3 Results

System Function

The system function is the same as chapter two; as a result the responses are identical. Ice is nucleated on the surface of the probe and progresses outward in a radial direction after a period of time, which is usually 30-60 seconds. Progression of the ice front in the radial direction occurs until the liquid nitrogen source is removed, although near the end of the freezing cycle, the rate of ice growth slows dramatically. Rings of differing shades of white-grey may form within the ice-ball. In some cases small cracks form within the ice-ball, usually within the first half of the ice-ball closest to the probe. By termination of freeze, the ice-ball covers roughly ¾ of the chamber's radius, but does not reach the edge that is maintained at 37°C. The duration of the thawing process is quite long, with the ice in the middle taking the longest to thaw for a duration of 25 minutes. Examples of temperature profiles for the single and double freeze-thaw cycles are seen in figures 3.1 and 3.2 respectively. The single freeze-thaw graph looks identical to the single freeze-thaw graph of methocel in chapter 2 (figure 2.7), and there are no differences with the addition of cells in suspension. The graph of the double freeze-thaw cycle is quite similar to the single freeze-thaw

cycle, the only difference is that there are two profiles. Both of the freezes within the double freeze-thaw cycle highly resemble the single freeze-thaw profile.

Syto/EB

The appearance of the membrane intact controls stained with Syto/EB is characterised by green fluorescence. All of the nuclei are well formed and intact. With the non-intact control all cells in the sample are red. The nuclei appear to be abnormal in appearance.

A graph of membrane integrity versus radial distance from the probe in figure 3.3 shows the variability in response of cells to freezing using a single freeze-thaw protocol. Those cells closest to the probe have 85-100% loss of membrane integrity, while those approximately half way in the ice-ball have 60-80% loss of membrane integrity. It is important to note that 50-60% of the cells within the last third of the ice-ball still have intact membranes.

The graph in figure 3.4 shows the variability in response of cells to a double freeze-thaw protocol. In this case, the cells within the first two thirds of the ice-ball closest to the probe react the same as the single freeze-thaw protocol. The cells in the last third of the ice-ball, closest to the periphery maintain approximately 30% membrane integrity. Statistical analysis of these results indicates that there is a statistically significant difference between the two freezes in the outer portion of the ice-ball ($p \leq 0.001$). There are no statistical differences between the EB results of the two protocols in the middle or interior of the ice-ball closest to the probe. A numerical comparison of Syto/EB results from both freezes is given in table 3.1.

AlamarBlue

The samples in the 96 well plates are different colours. Those samples biopsied from sites close to the cryoprobe remained dark blue in colour, similar to the negative control with dead cells and the negative control with just the alamarBlue and methocel. The negative controls do not change in absorbance throughout the entire experiment. Those samples biopsied from the middle part of the ice-ball (between the area closest to the probe and the periphery) turn a light purple in colour. Those cells in the periphery of the ice-ball turn bright pink in colour, not quite as bright as the positive control with 100% viability.

A graph of the percent alamarBlue reduced with respect to distance from the probe is presented in figure 3.5 for both the single and double freezes. There are no significant differences between the two freezes at distances close to the cryoprobe, however a significant difference occurs at the outer edge of the ice-ball. A comparison of the calculated percent viability for the double and single freezes using alamarBlue and EB is presented in figures 3.6 and 3.7. The double freeze-thaw comparison shows little difference between the EB and alamarBlue data. The single freeze comparison differs at the very last thermocouple where percent of non-viable cells with alamarBlue is 0% and with EB is 39%.

Cooling Rate and End Temperature Effects

The results of cooling rate and end temperature versus viability are given in table 3.2 for the single freeze-thaw protocol. Table 3.3 shows the results of double freeze-thaw protocols for cell viability versus cooling rate and end temperature. All end temperature and cooling rate data are taken from the

temperature versus time profiles for each freeze recorded by the data acquisition system.

3.4 Discussion

In the literature there is an abundance of information about the effects of single and double freeze protocols for entire tissues or cells in suspension. However, there is insufficient information concerning individual cell survival at various distances, temperatures and cooling rates within tissues. The purpose of this chapter is to examine the most basic and common cryosurgical procedures, the single and double freeze-thaw protocols respectively, and determine biological reactions of cells in a model tissue system to freezing. This includes establishing rates of cell kill at various distances, cooling rates, temperatures from the cryoprobe, number of cycles, and duration of freeze.

In a cryosurgical ice-ball, the cells closest to the probe experience the fastest cooling rates, lowest temperatures and longest duration of freeze. For these reasons, the highest rates of kill are seen here. The cells in the middle of the ice-ball undergo intermediate temperatures and cooling rates, but also have intermediate rates of cell kill. Cells at the periphery of the ice-ball undergo the slowest rates of cooling and highest temperatures, resulting in the lowest rates of cell kill.

The cooling rate plays an important role in freezing damage due to the increase in intracellular ice formation at fast cooling rates, which is considered lethal (9). Studies have shown that intracellular ice forms near the cryosurgical probe, but closer to the periphery cells look shrunken and dehydrated. Cooling

rates of 50°C/min or faster are common in the area closest to the cryosurgical probe in actual cryosurgical procedures (7,8). The cooling rates in the cryosurgical model system fall within this range. The data for the single freeze-thaw protocol show that there is a significant increase in cell kill to about 80% at cooling rates faster than 45-50°C/min. In the double freeze-thaw experiments we see the same increase in cell kill to 80% but at cooling rates only around 30°C/min. Both of these occur approximately 10 mm from the probe. According to these results, using a double freeze-thaw protocol may effectively decrease the cooling rates necessary to kill the same amount of cells. If this is the case, one might speculate that the increase in time at subzero temperatures increases the damage to cells. Gage found that this is true when freezing dog epithelium, the longer the holding temperature, the more damage there is to cells. This holds true especially at warmer sub-zero temperatures, however it is not thought to contribute significantly at temperatures colder than –50°C since most of the water is frozen at this point. More than likely, the double freeze increases the likelihood of intracellular ice formation, since the probability of intracellular ice formation increases with exposure time (16). Statistical analysis of the region closest to the probe shows that there is no statistically significant difference in the rates of cell kill.

It is also noteworthy that the cooling rates are different in the two protocols; for the first three thermocouple sites closest to the probe there is a significant increase in cooling rate. The difference in cooling rates seems to be important closest to the probe and dissipates within the first four thermocouples.

The last six sites in both the single and double freeze experience the same cooling rates. It is in this outer area, where the cooling rates and end temperatures are the same, that there is a statistically significant increase in cell kill ($p \leq 0.001$) in the double freeze-thaw protocol. This increase in cell kill may be associated with more time spent at the low sub-zero temperatures. It has been demonstrated that at low sub-zero temperatures between 0 and –30°C, damage due to solution effects increases with a corresponding increase in time spent at these temperatures (11,17). Cells are exposed to increased concentrations of solutes that become increasingly deleterious with continued exposure.

In cryosurgery, cancer cells are eradicated with the use of cold temperatures. Many studies have shown that each cell type has its own temperature threshold, below which all cells die (1,10,18). Therefore if all the cells within a tumour can be frozen below or to this level, all the cells will die. Theoretically this is possible, but *in vivo* it becomes much more difficult when you consider the location of tumours and their heterogeneous composition. The temperatures at which normal cells die tend to be warmer than those temperatures required by neoplastic cells since they seem to be more resistant (19,20,21). Animal studies *in vivo* have shown that temperatures between –20 to –30 in the form of a single freeze-thaw cycle are sufficient to kill all cells within the ice-ball (22,23). Other studies of the same kind show destruction, but cell kill is not 100% (24,25). Some cells, especially in the periphery of the ice-ball do survive the freezing process. Other studies have shown that temperatures in the range of –60 to –70°C are necessary to guarantee cell destruction, and more

than one freeze-thaw cycle is necessary (12). The experiments in this chapter tend to confirm the later findings with temperatures of –60 to –65°C resulting in 80% cell kill. From a purely cryobiological aspect, direct cell injury as a result of the freezing and thawing processes that results in 100% cell kill, is not seen until tissue temperatures reach –100°C for both protocols. It is thought that a large part of the damage is actually contributed by secondary factors such as anoxia resulting from vascular stasis, which may decrease the necessary amounts of cell kill from purely cryobiological aspects (2). How much each aspect contributes to kill is unknown. Therefore, 100% cell kill by cryobiological aspects is not possible since these temperatures only exist within the first half a centimetre from the probe. One disadvantage of using this model system is the inability to look at long term effects of freezing and vascular stasis.

One interesting note about the freezing process during cryosurgery that has not been investigated in the past, is what happens to the cells at the exterior of the ice-all that do not actually freeze. The periphery of the ice-ball is characterised by 20% cell kill at an average end temperature of 0°C in the single freeze protocol, whereas 60% of the cells are killed at an average end temperature of 15°C in the double freeze-thaw protocol. Obviously none of the cells are frozen in either case and damages arise from something other than direct freezing injury. Hypothermic damage could be the source, since it can alter cell function and physiology (27). The cells are not at these temperatures for very long, and since this type of damage typically takes time to develop, the assumption is made that hypothermic damage is not the key factor causing cell

death. More likely, the source of damage is osmotic pressure. As ice forms at the front of the ice-ball, water is removed from solution and increases in concentration occur in front of the frozen portion. These increases in concentration can have deleterious effects on cells depending on the concentration and time of exposure. Cells in this unfrozen hypertonic region suffer from solute exposure and in the double freeze protocol, they go through this process twice.

One other theory could explain the increase in damage. Damage could be caused by the changes in concentration, rather than by the concentration itself. This is supported by Lovelock's and Farrant's work which show that post hypertonic damage, otherwise known as dilution shock occurs as a result of excessive water entry due to the increase in intracellular solute concentrations (26,27). This can occur in the absence of freezing by using hypertonic solutions alone.

More tissue destruction is caused by using a double freeze protocol since cells must undergo the freezing and thawing process twice (1). Each time they pass through temperatures that cause injury, this adds to the effects of freezing damage. The experimental results suggest that increasing the number of freeze-thaw cycles will increase the injury to cells. Theoretically one could perform three or more freeze-thaw cycles, but in practicality this would probably kill the patient. Increasing the number of freeze-thaw cycles *in vivo* alters the tissue structure and increases the thermal conductivity resulting in a greater volume of freeze (28). Also documented is increased tissue destruction, better cure rate, larger

intracellular ice crystals, and a movement of necrosis closer to the border of the lesion (24). The experiments in this chapter confirm many of these statements. Although not examined in this study, increased intracellular ice formation could explain the increased amounts of cell kill in the outer portion of the ice-ball. This is possible since intracellular ice formation is more likely to form with repeated cycles and the ice crystals tend to be larger (3). Also important is the warming step in the protocol since cells would undergo the effects of recrystallization twice. Another consideration is that cells spend twice the amount of time at injurious temperatures, an important factor when considering damage from solution effects which is present in these temperature ranges.

A realistic cryosurgical model system enabling exact temperature measurements and tissue biopsy sites in a tissue representative size model has not been developed until now. This novel system takes into consideration most of the realistic factors present with an *in vivo* system but allows study of individual cells within a model tissue. The results from the single and double freeze protocols give a good indication of what happens to cells on a basic cryobiological level and as a result of freezing injury alone. It is quite evident that a single freeze-thaw cycle is insufficient when considering this treatment for cancer. The lack of damage to the outer portion of the ice-ball is very obvious and the simple task of performing a second freeze cycle results in a two times increase in cell kill at the periphery of the ice-ball. This effect is more than likely a combination of many factors that include duration of freeze and being subjected twice to the same damaging events.

3.5 References

1. Gage, A. Review: Mechanisms of tissue injury in cryosurgery. *Cryobiology* **37**, 171-186 (1998).
2. Rubinsky, B., Lee, C., Bastacky, J. and Onik, G. The process of freezing and the mechanism of damage during hepatic cryosurgery. *Cryobiology* **27**, 85-97 (1990).
3. Whittaker, D. Mechanisms of tissue destruction following cryosurgery. *Annals of the Royal College of Surgeons of England* **66**, 313-318 (1984).
4. Baust, J. and Chang, Z. Underlying mechanisms of damage and new concepts in cryosurgical instrumentation. *In* "Cryosurgery: Mechanism and applications." Pp. 21-36. International Inst. Refrigeration, Paris, France, 1995.
5. Gage, A., Guest, K., Montes, M., Caruana, J. and Whalen, D. Effect of varying freezing and thawing rates in experimental cryosurgery. *Cryobiology* **22**, 175-182 (1985).
6. Zacharian, S. The observation of freeze-thaw cycles upon cancer cell suspensions. *J. Dermatol. Surg. Oncol.* **3**, 173-174 (1977).
7. Bischof, J., Merry, N., and Hulbert, J. Rectal protection during prostate cryosurgery: design and characterization of an insulating probe. *Cryobiology* **34**, 80-92 (1997).
8. Bischof, J., Smith, D., Pazhayannur, P., Manivel, C., Hulbert, J., and Roberts, K. Cryosurgery of Dunning AT-1 rat prostate tumor: thermal,

biophysical, and viability response at the cellular and tissue level. *Cryobiology* **34**, 42-69 (1997).

9. Mazur, P. A role of intracellular freezing in the death of cells cooled at supraoptimal rates. *Cryobiology* **14**, 251-272 (1977).
10. Gage, A., Caruana, J., and Montes, M. Critical temperature for skin necrosis in experimental cryosurgey. *Cryobiology* **19**, 273-282 (1982).
11. Mazur, P. Freezing of living cells: mechanisms and implications. *Am. J. Physiol.* **247**, 125-142 (1984).
12. Gage, A. Experimental cryogenic injury of the palate: Observations pertinent to cryosurgical destruction of tumours. *Cryobiology* **15**, 415-425 (1978).
13. Stewart, G. Preketes, A., Horton, M., Ross, W. and Morris, D. Hepatic cryotherapy: Double-freeze cycles achieve greater hepatocellular injury in man. *Cryobiology* **32**, 215-219 (1995).
14. Whittaker, D. Repeat freeze cycles in cryosurgery of oral tissues. *Brit. Dent. J.* **139**, 459-464 (1975).
15. BioSource International. AlamarBlue™ assay. Package insert.
16. Meryman, H. Freezing injury and its prevention in living cells. *Annu. Rev. Biophys.* **3**, 341-363 (1974).
17. Mazur, P., Leibo, S. and Chu, E. A two-factor hypothesis of freezing injury. *Exptl. Cell Res.* **71**, 345-355 (1972).
18. Neel, H., Ketcham, A. and Hammond. Requisites for successful cryogenic surgery of cancer. *Arch. Surg.* **102**, 45-48 (1971).

19. Jacob, G., Kurzer, M. and Fuller, B. An assessment of tumor cell viability after *in vitro* freezing. *Cryobiology* **22**, 417-426 (1985).

20. Heard, B. Nuclear crystals in slowly frozen tissues at very low temperatures: Comparison of normal and ascites tumour cells. *Br. J. Surg.* **42**, 659-663 (1955).

21. Tatsutani, K., Rubinsky, B., Onik, G. and Dahiya, R. The effect of thermal variables on frozen human prostatic adenocarcinoma cells. *Urology* **48**, 441-447 (1997).

22. Cozzi, P., Lawson, J., Lynch, W., and Morris, D. Critical temperature for *in vivo* cryoablation of human prostate cancer in a xenograft model. *Br. J. Urol.* **77**, 89-92 (1996).

23. Rivoire, M., Voiglio, E., Kaemmerlen, P., Morlina, G., Treilleux, I., Finzy, J., Delay, E. and Gory, R. Hepatic cryosurgery precision: Evaluation of ultrasonography, thermometry, and inpedancemetry in a pig model. *J. Surg. Oncol.* **61**, 242-248 (1996).

24. Dilley, A., Dy, D., Warlters, A., Copeland, S., Gillies, A., Morris, R., Gibb, D., Cook, T., and Morris, D. Laboratory and animal model evaluation of the Cryotech LCS 2000 in hepatic cryotherapy. *Cryobiology* **30**, 74-85 (1993).

25. Homasson, J.P., Thiery, J.P., Angebault, M., Ovtracht, L., and Maiwand, O. The operation and efficacy of cryosurgical, nitrous oxide-driven cryoprobe I Cryprobe physical characteristics: their effects on cell cryodestruction. *Cryobiology* **31**, 290-304 (1994).

26. Lovelock, J. The hemolysis of human red blood-cells by freezing and thawing. *Biochemica Et Biophysica Acta* **10**, 414-426 (1953).

27. Farrant, J. and Morris, G. Thermal shock and dilution shock as the causes of freezing injury. *Cryobiology* **10**, 134-140 (1973).

28. Gill, W., Fraser, J. and Carter, D. Repeated freeze-thaw cycles in cryosurgery. *Nature* **219**, 410-413 (1968).

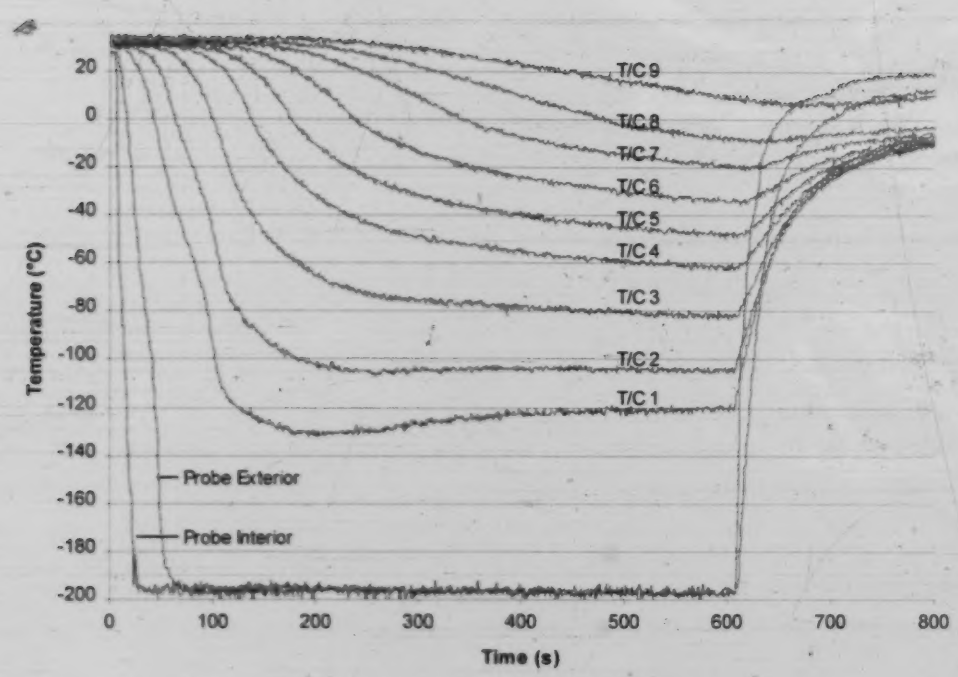

Figure 3.1 Example of a single freeze-thaw protocol with cells. The temperature profiles correspond to thermocouple measurements taken in the chamber. The first two curves on the bottom of the graph represent the temperatures inside and outside the probe. The other curves are the freezing profiles of methocel with increasing distance from the probe.

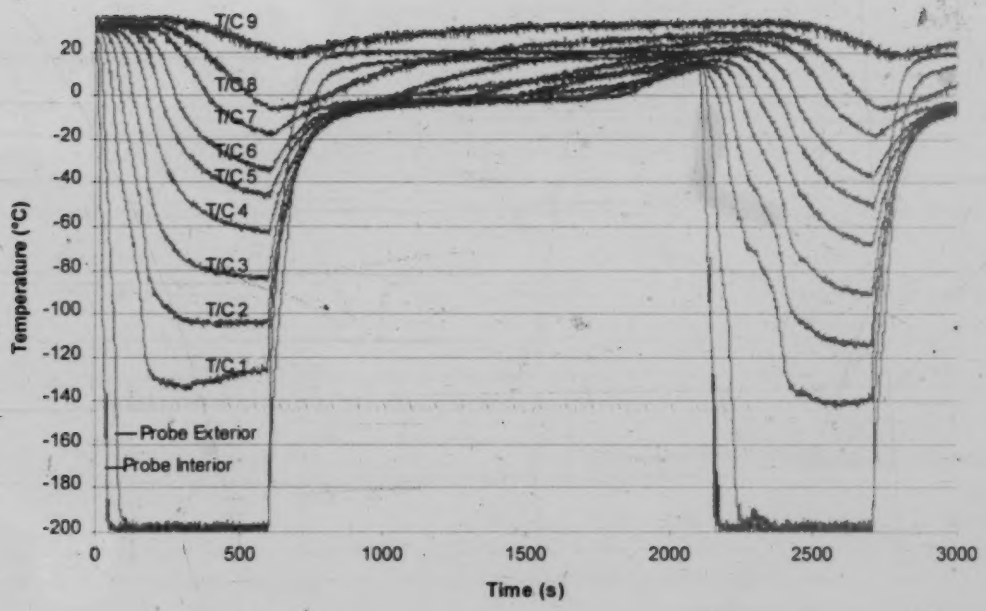

Figure 3.2 Example of a double freeze-thaw protocol with cells. The temperature profiles correspond to thermocouple measurements taken in the chamber. The first two curves on the bottom of the graph represent the temperatures inside and outside the probe. The other curves are the freezing profiles of methocel with increasing distance from the probe.

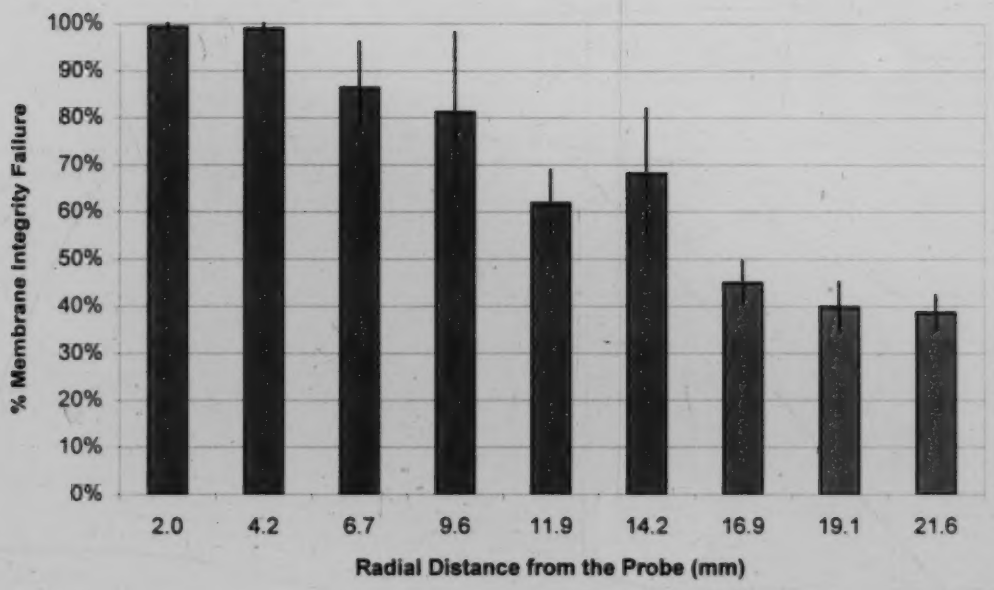

Figure 3.3 Membrane integrity staining results for the single freeze-thaw protocol with respect to radial distance from the probe.

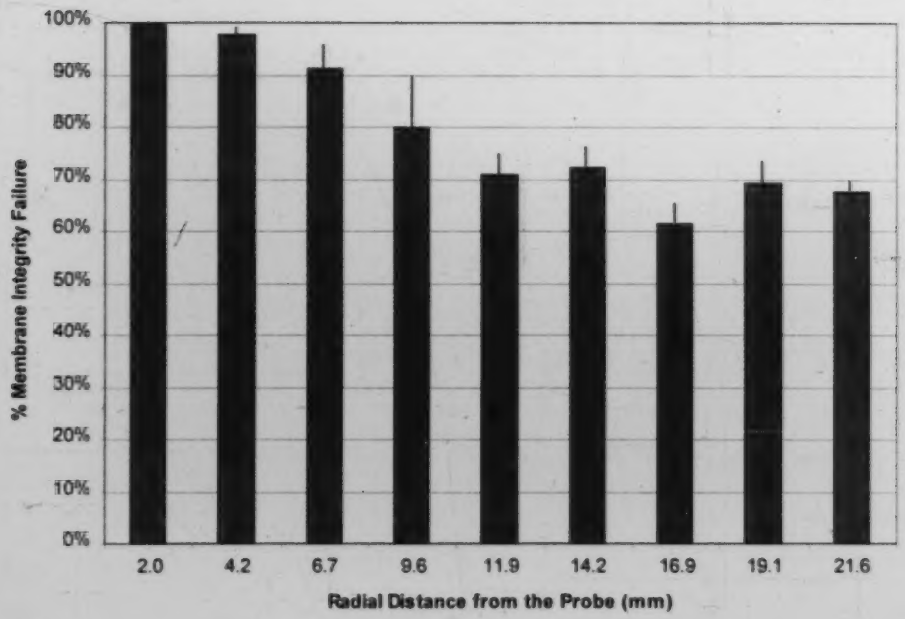

Figure 3.4 Membrane integrity staining results for the double freeze-thaw protocol with respect to radial distance from the probe.

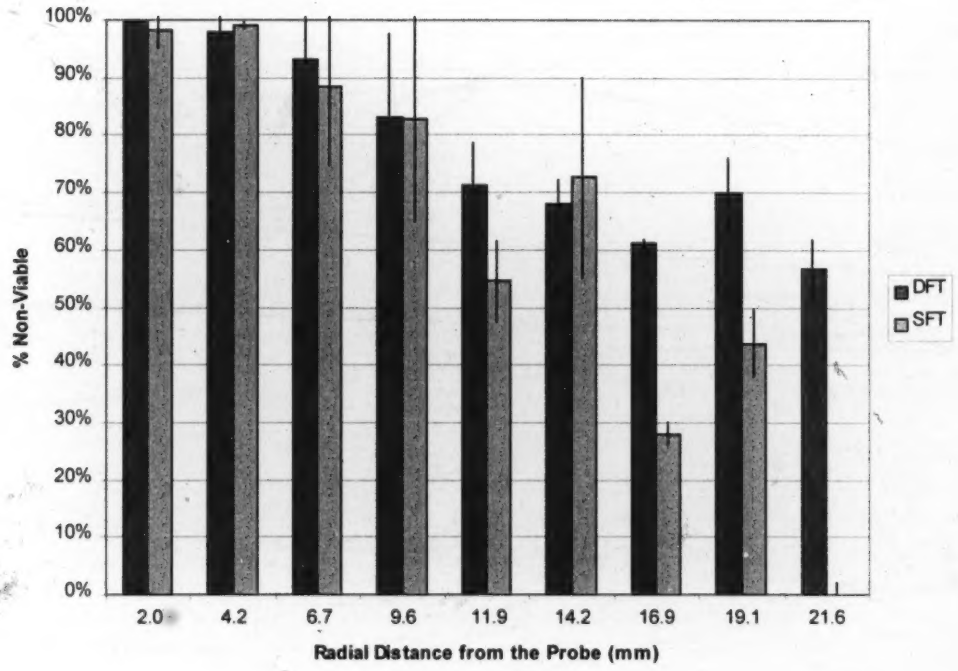

Figure 3.5 Comparison of cell viability for the single and double freeze-thaw protocols with respect to distance from the probe using alamarBlue where SFT represents the single freeze-thaw and DFT the double freeze-thaw.

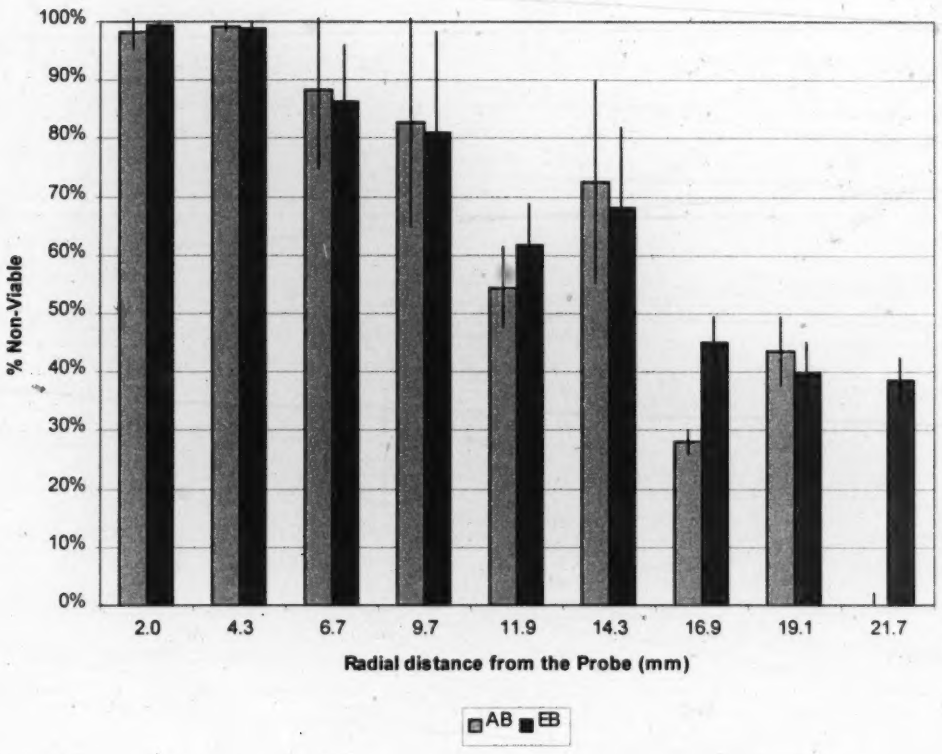

Figure 3.6 Viability comparison of Syto/EB versus alamarBlue at various distances from the probe for the single freeze-thaw protocol.

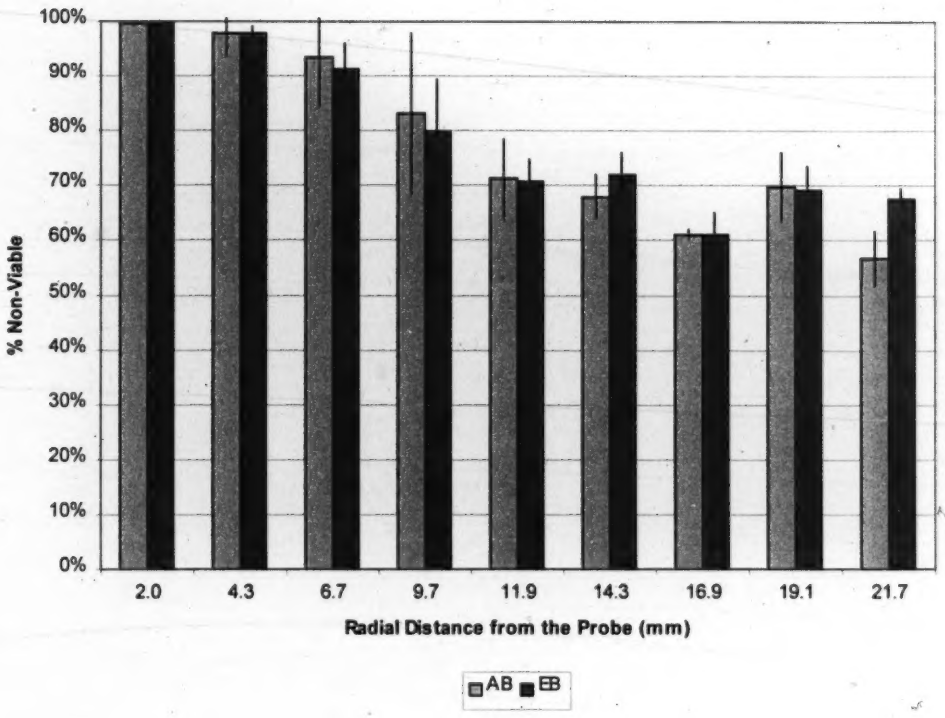

Figure 3.7 Viability comparison of Syto/EB versus alamarBlue at various distances from the probe for the double freeze-thaw protocol.

Radius (mm)	Single Freeze-thaw (% intact)	Double Freeze-thaw (% intact)
2.0	1 ±1	0 ±0
4.3	1 ±1	2 ±1
6.7	14 ±10	9 ±5
9.7	19 ±17	20 ±10
11.9	38 ±7	29 ±4
14.3	32 ±14	28 ±4
16.9	55 ±5	39 ±4
19.1	60 ±5	31 ±5
21.7	61 ±4	32 ±2

Table 3.1 Comparison of Syto/EB results for the single and double freeze-thaw protocols with respect to distance from the probe.

Radius (mm)	Cell Death (%)	Cooling Rate (°C/min)	End Temperature (°C)
2.0	99 ±2	121	-134
4.3	99 ±1	95	-106
6.7	87 ±12	67	-80
9.7	82 ±17	45	-59
11.9	58 ±7	33	-46
14.3	70 ±15	23	-32
16.9	36 ±3	15	-21
19.1	42 ±6	10	-11
21.7	19 ±3	7	0

Table 3.2 The results of cooling rate and end temperature versus viability for the single freeze-thaw protocol. Radius is the distance from the probe, cell death is the percent of non-viable cells represented by averages of Syto/EB and alamarBlue together.

Radius (mm)	Death (%)	Rate 1 (°C/min)	Rate 2 (°C/min)	Temp 1 (°C)	Temp 2 (°C)
2	100 ±0	59	57	-138	-145
4.3	98 ±3	51	48	-109	-118
6.7	92 ±7	42	39	-87	-96
9.7	81 ±12	33	30	-66	-73
11.9	71 ±6	27	23	-48	-54
14.3	70 ±4	21	20	-34	-39
16.9	61 ±2	16	15	-17	-20
19.1	69 ±5	11	12	-5	-8
21.7	62 ±3	6	7	17	15

Figure 3.3 Results of double freeze-thaw protocols for cell viability versus cooling rate and end temperature. Radius is the distance from the probe in mm. Death is the average of alamarBlue and Syto/EB percent non-viable cells after freezing. Rate 1 and rate 2 refer to the fastest cooling rates in degrees per minute for the first and second freeze of the double freeze-thaw respectively. Temp 1 and temp 2 are the coldest end temperatures in °C reached during the freeze at each thermocouple in the sample.

CHAPTER 4: TEMPERATURE CYCLING

4.1 Introduction

Investigations in cryosurgery are typically grouped in two ways, the first group consists of clinical studies that examine tumour cell death in tissue as a whole or measure cell death by recurrence of the malignancy. The second group is comprised of studies on the basics of cryosurgical injury and cell death. There is a need for both sides to work together using their knowledge to improve cryosurgery.

The effectiveness of the double freeze-thaw protocol is undisputed in cryosurgery. However, conflicting responses to the double freeze-thaw protocol in clinical liver and prostate cryosurgery have led to its disuse in some cases. Previous use of the double freeze-thaw technique has led to severe complications, even death in some cases (1,2). Some surgeons are opting for a double freeze cycle approach that involves freezing the tissue, but not thawing the ice-ball until it has completely melted before refreezing (1,3). Other surgeons have not experienced the problems associated with double freeze-thaw techniques and continue to use this protocol (4).

No direct comparison has been performed between these two protocols to determine what effect the differences have on cell viability within a tissue with respect to distance from the probe. Information on altering cell viability due to differences in temperature, cooling rates, and duration of freezing and thawing would be useful to determine which protocol is better. If cellular responses are altered due to changes in the freeze-thaw protocols, it is as a result of changes to the thermal histories. Thermal history relates directly to the amounts and types of injury incurred

by cells, but these changes have not been explored in the past. This chapter will investigate the effects of temperature cycling, examining the consequences in the form of viability results and changes to thermal profiles. The purpose of these studies is to provide more quantitative data correlating thermal history to viability. These experiments will be used to compare a double freeze cycling protocol that is in practical use during actual cryosurgical procedures with a new triple freeze cycle technique and determine their effectiveness. The effectiveness of cycling protocols will also be compared to the single and double freeze-thaw results from chapter 3.

Increasing the number of repeated cycles causes more damage to tissues (5,6,7,8), but triple freeze-thaw protocols are not used clinically due to the complications that are expected. Researchers in the field of cryosurgery have indicated that a triple freeze-thaw cycle will probably kill the patient, so this is not an option. If the double freeze cycle leads to less complications *in vivo*, perhaps the triple freeze cycle will increase the effectiveness of cryosurgery but decrease the rate of complications when compared to the triple freeze-thaw cycle.

No one has looked closely at temperature cycling, but it is important to understand since increasing the number of freeze-thaw cycles kills more cells in the periphery of the ice-ball. In a clinical setting, the highest number of surviving malignant cells are located in this area (9,10). Using more cycles seems like the ideal solution to treat those cells that tend to survive in the periphery of the ice-ball. Unpublished evidence from our lab has shown that complete thawing in between freezing cycles is not necessary for damage to accumulate when cycling between two sub-zero temperatures. The extent of this damage compared to single and

double freeze-thaw protocols is unknown. It is suspected that the increase in cellular injury is a result of constantly changing osmotic fluxes within the cells in response to their changing environment.

The results of these experiments can be used in determining better treatment planning for patients. Benefits to the patient include increased cell kill in the periphery of the ice-ball without increasing the time in surgery or complication rates.

4.2 Methods and Materials

Cell Culture

Tissue culture is performed as mentioned previously in chapter 2. In summary, the PC3 cell line is grown in F-12K nutrient mixture supplemented with 7% v/v FBS and 1 mg/L penicillin-streptomycin at 37°C in an atmosphere of 95% air and 5% CO_2. Cells are grown in 75 cm^2 flasks (Corning Glass Works, Corning, NY) and trypsinized when near confluent using 0.25% trypsin with EDTA (all tissue culture elements from GIBCO Laboratories, Grand Island, NY). After the cells are detached, they are resuspended in media and counted. The cell concentration is adjusted to approximately 1.1 X 10^6 cells/ml for all experiments.

Media Preparation

The methocel is stored in a –20°C freezer and when it is needed, immersed in a water bath until it reaches 37°C. At this point, 9.1 ml of cell suspension at a concentration of 1.1 X 10^6 cells/ml is mixed well into 20.9 ml 37°C methocel. A vacuum is then attached to the cell-methocel suspension while remaining in a 37°C water bath for a period of 1 hour, until all trapped air bubbles are out of the

methocel. The heater that maintains the cryosurgical system at 37°C is turned on, and then the mixture is added and the experiment begins.

Cryosurgical System and Freezing Protocols

The cryosurgical system is the same as described in chapter 2 of this thesis. Freezing can begin once the cells and medium are added to the system. The liquid nitrogen source and temperature monitoring devices are activated after the lid and supply hoses are secured into place. The double freeze cycle protocol consists of 10 minutes of continuous uninterrupted freezing. Liquid nitrogen flow is arrested at this point, and the sample is warmed using room temperature air flowing through the supply tube until the coldest temperature within the cryosurgical system reaches approximately –10°C, taking around 9 minutes to accomplish. The methocel is frozen for a period of 6 minutes the second time. When the ice-ball reaches the same size as the first freeze, the system is warmed for approximately 25 minutes using room temperature air. This allows the methocel and thermocouples to reach room temperature. The triple freeze cycle involves an extra 9 minute thaw and 6 minute freeze in addition to the double freeze cycle.

Samples are removed from the chamber when the interior of the chamber reaches room temperature, using 19 gauge 1½ (3.81 cm) inch needles and 1 ml syringe through the biopsy sites. One 200 µl sample is removed from each biopsy site (9 from the system plus 2 controls). The samples are incubated for 1 hour at 37°C in 5% CO_2 and used in assays to determine viability. The positive control consists of cells in methocel biopsied from the system before freezing and viability is approximately 100%. The negative control consists of cells in methocel biopsied

before freezing and subjected to 15 freeze-thaw cycles to kill all the cells. There is zero percent cell survival as measured by a lack of membrane integrity and inability to metabolise alamarBlue.

Syto/EB

The Syto/EB is prepared and used in the same manner as described in chapter 3. Membrane integrity is evaluated 1 hour post-thaw after mixing 100 µl of the cell suspension with 20 µl of Syto/EB and allowing 5 minutes for the dye to penetrate the cells. Cells are counted under dual fluorescent-brightfield illumination using a hemocytometer (Reichert Scientific Instruments, Buffalo, NY) and an Axioskop microscope (Carl Zeiss Inc. Germany). For each experiment, 4 counts are made from each biopsy site.

AlamarBlue

The remaining 100 µl of cell suspension and 10 µl of alamarBlue are added to a 96 well plate (Corning Glass Works, Corning, NY) and incubated at 37°C in 5% CO_2 for 2.5 hours. The absorbance is read using a UV Max microplate reader (Molecular Devices Corporation, Menlo Park, CA) at 570 and 600 nm. The percent of alamarBlue reduced is calculated using a formula provided by the manufacturer to compensate for the overlapping spectra at 570 and 600 nm (11). The number of viable cells can be found using the standard graph from chapter 2 and the equation derived from this graph. Knowing the percent reduction allows calculation of the number of cells that are alive. The number of dead cells can be deduced from the fraction of cells remaining from the original cell concentration.

4.3 Results

System Function

Ice forms on the surface of the probe, progressing in the radial direction until the liquid nitrogen source is removed. Near the end of the freezing cycle, the rate of ice growth slows dramatically. Rings of differing shades of white-grey may form within the ice-ball. In some cases small cracks form within the ice-ball, usually within the first half of the ice-ball closest to the probe. By termination of freeze, the ice-ball covers roughly ¾ of the chamber's radius, but does not reach the edge that is maintained at 37°C. The duration of thaw is approximately 9 minutes. After the 9 minute thaw, the periphery of the ice-ball is slightly thawed, as is the area closest to the probe. Most of the ice-ball remains in the frozen state. Examples of temperature profiles for the double and triple freeze cycles are seen in figures 4.1 and 4.2 respectively. The first freeze of the double freeze cycle looks identical to the first freeze of the double freeze-thaw protocol. The second freeze of the double freeze cycle is not the same. The slight waviness of the first freeze is not apparent in the second freeze in the cycling graphs and the second set of temperature profile curves is much steeper. The triple freeze cycle graph is identical to the double freeze cycle only there is an additional steep, non-wavy temperature profile. It is likely that the differences in profiles after the first freeze are because no latent heat is produced.

Syto/EB

The appearance of the membrane intact controls stained with Syto/EB is characterised by green fluorescence. All of the nuclei are well formed and intact.

With the non-intact control all cells in the sample are red. The nuclei appear to be abnormal in appearance.

A graph of membrane integrity versus radial distance from the probe in figure 4.3 shows the variability in response of cells to freezing using a double freeze cycle protocol. The only area of complete necrosis is within the first two biopsy sites radially from the probe. The middle two thirds of the ice-ball average about 67% kill and the periphery 50% kill.

The graph of membrane integrity in figure 4.4 shows the variability in response of cells to a triple freeze cycle protocol with respect to distance from the probe. Notice that the area of complete necrosis extends through the first 10 mm radially from the probe. The rest of the ice-ball is quite variable in terms of membrane integrity. Statistical analysis of the double and triple freeze cycle protocols shows that there is a statistically significant difference between the two freezes only at the third thermocouple from the probe. Any other differences in the rest of the ice-ball are due to random sampling differences and are inconsequential. A numerical comparison of the Syto/EB results from both freezes is presented in table 4.1.

AlamarBlue

The samples in the 96 well plates are different colours. Those biopsies from areas close to the cryoprobe remain dark blue in colour and do not change in absorbance throughout the experiment, the same as the negative controls with dead cells with just alamarBlue and methocel. Those biopsies from the middle of the ice-ball (between the area closest to the probe and the periphery) turn a light purple in

colour. Cells in the periphery of the ice-ball turn bright pink in colour, but not quite as bright as the control with 100% membrane intact cells.

A graph of the percent alamarBlue reduced with respect to distance from the probe is presented in figure 4.5 for both the double and triple freeze cycles. There are no significant differences between the two freezes in the cells at the periphery of the ice-ball or in the cells close to the probe. The only significant differences are at thermocouples 6.7 and 14.25 ($p<0.05$). A comparison of the calculated percent viability for the double and triple freeze cycles using alamarBlue and EB is presented in figures 4.6 and 4.7. The double freeze cycle comparison shows little difference between the EB and alamarBlue data except at the very last thermocouple where the alamarBlue is 7% and the EB is 45%. The triple freeze cycle comparison differs at the very last thermocouple and at 14.25 mm where the percent of non-viable cells with alamarBlue is 20% lower than with EB.

Cooling Rate and End Temperature Effects

The results of cooling rate versus viability for the double and triple freeze cycle protocols are given in tables 4.2 and 4.3 respectively. Tables 4.4 and 4.5 are the findings of the end temperatures reached for the double and triple freeze cycling respectively. All end temperature and cooling rate data originate from the temperature versus time profiles for each freeze by the thermocouples attached to the data acquisition system.

4.4 Discussion

There is a lack of information about temperature cycling in cryosurgery. What information is available remains limited. There have been no direct comparisons

between the double freeze-thaw and double freeze cycle protocols to determine the exact effects of these techniques on individual cell viability with respect to distance from the probe. Temperature, cooling rates, and time spent during freezing and thawing all contribute to the viability of cells after freezing (12,13,16), but none of these factors have been examined within this context.

When the end temperatures are examined for all freezes, there are no significant differences between them. The distribution of temperatures within the ice-ball is standard by the end of the freezing cycle. Examination of cooling rates shows that all of the first freezes in the double freeze-thaw, double freeze cycle and triple freeze cycle protocols have the same rates. The cooling rates in the single freeze-thaw protocol are much higher rate within the first four thermocouples adjacent to the probe. Therefore, end temperatures are the same regardless of cooling rate within the sample.

The viability results are quite different even though temperatures are the same. The single freeze-thaw, double freeze-thaw, and triple freeze cycle have very similar rates of kill in the first four biopsy sites closest to the probe, close to 100% cell death. The double freeze cycle has 40% viability for the 6.7 and 9.65 mm sites even though they are at the same temperatures as each other. These are statistically significant differences ($p=0.038$). Therefore, other influences may be at play.

In the case of the single freeze-thaw protocol, the cells are not subjected to lower subzero temperatures, increased time at subzero temperatures, nor do they pass through damaging subzero temperatures twice. Therefore, the major factor

involved in the increase in cell kill is more than likely due to the increase in cooling rate. This is reinforced by the fact that the cooling rates are much higher only near the probe where the increase in cell kill occurs. At the periphery of the ice-ball in the single freeze-thaw cycle where the cooling rate returns to normal, there is no increase in cellular destruction.

The temperatures and cooling rates for all freezes in the double and triple freeze cycle protocols are the same, and yet the triple freeze cycle kills a statistically significant increased number of cells in sites located at 6.7 and 9.65 mm. One factor that could be responsible for this is an increase in the number of cycles. This cycles cells more times through the temperatures and cooling rates that have deleterious effects. The other factor could be the increased time at subzero temperatures, which has been shown to increase damage to cells (12). This is not as likely though, since the temperatures at which this increase in damage occurs normally are warmer than –50°C. The temperatures at which increases in injury occurs are colder than this.

At intermediate distances from the probe, only one site has significant differences in cell kill. At 16.9 mm from the probe there is a statistically significant difference between the cycling protocols and the single freeze-thaw protocol ($p=0.03$). Previous research has shown that increasing the amount of time spent at sub-zero temperatures increases damage (13). At temperatures below –50°C this effect is not pronounced since all water is frozen (12). The temperature at this biopsy site is –20°C, and the increase in holding time should increase injury to cells due to solution effects. In previous research the –20 to –30°C range increases damage to cells. In this region, repeated freeze-thaw cycles lead to an increase in intracellular

ice (5). In this set of experiments, the repeated freeze cycling at this temperature may lead to an increase in intracellular ice and could explain the significant increase in damage.

The double freeze-thaw is just as effective at killing cells close to the probe as the triple freeze cycle but only traverses the injurious temperature zones twice. These results show that the effects of complete thawing may be important in the development of damage. It could be that complete thawing takes advantage of the entire range of recrystallization temperatures. This is very likely since we know that intracellular ice forms in this region where cooling rates are still high and temperatures are low. Another reason for the increase in cell death could be injury from dilution shock after rapid freezing as proposed by Farrant and Lovelock (14,15). The cells are exposed to hypertonic solutions while thawing that lead to dilution shock when ice melts.

It is important to note that the double freeze-thaw protocol is the most effective at reliably killing cells in the periphery of the ice-ball with a statistically significant difference ($p \leq 0.001$) when compared to all other protocols. At 21.65 mm distance from the probe, the rate of cell kill is 62%. This is very significant since the temperatures in this region are well above freezing at 16°C on average and cooling rates of only 6°C/min. One possible explanation for this is the accumulation of solutes in advance of the freezing front. Cells that are located within this region remain unfrozen and suffer from exposure to high solute concentrations. Looking at the exposure time for the double freeze-thaw and the triple freeze cycle, exposure is greater in the triple freeze-thaw protocol. An alternative mechanism must be at work.

Damage could be caused by the changes in concentration, rather than by the concentration itself. This is supported by Lovelock's and Farrant's work which show that post hypertonic damage, otherwise known as dilution shock occurs as a result of excessive water entry due to the increase in intracellular solute concentrations (14,15). This occurs in the absence of freezing by using hypertonic solutions alone.

When interpreting the results of these experiments, keep in mind that *in vivo* cryosurgery kills all the cells in the centre of the ice-ball closest to the probe. The problem exists at the periphery of the ice-ball; with increasing distance from the probe more cells survive. The results of temperature cycling experiments show that they are more effective at killing cells in the periphery of the ice-ball when compared to the single freeze-thaw protocol. The double and triple freeze cycle protocols do not result in an increase in cell kill over the double freeze-thaw protocol at the periphery. In conclusion, the double freeze-thaw protocol is the most effective due to its ability to kill cells in the periphery of the ice-ball where cancer cells are most likely to survive. The importance of completely thawing the ice-ball in increasing the effectiveness of cryosurgery is well documented here. As a result of these experiments more information is known about temperature cycling and its lack of efficiency at killing cells at the periphery of the ice-ball when compared to the double freeze-thaw protocol.

4.5 References

1. Chuang, C., Chu, C., Chiang, H. and Chou, C. Application of cryoablation in the management of prostate cancer. *Chang Gung Med. J.* **20**, 201-206 (1997).
2. Lee, F., Mahvi, D., Chosy, S., Onik, G., Wong, W., Littrup, P. and Scanlan, K. Hepatic cryosurgery with intraoperative US guidance. *Radiology*. **202**, 624-632 (1997).
3. Sklar, G., Koschorke, G., Filderman, P., Naslund, M. and Jacobs, S. Laparoscopic monitoring of cryosurgical ablation of the prostate. *Surg. Lap. Endo.* **5**:5, 376-381 (1995).
4. Lee, F., Bahn, D., McHugh, T., Onik, G. and Lee Jr., F. US-guided percutaneous cryoablation of prostate cancer. *Radiology* **192**, 769-776 (1994).
5. Whittaker, D. Mechanisms of tissue destruction following cryosurgery. *Annals of the Royal College of Surgeons of England* **66**, 313-318 (1984).
6. Gage, A. Experimental cryogenic injury of the palate: Observations pertinent to cryosurgical destruction of tumours. *Cryobiology* **15**, 415-425 (1978).
7. Stewart, G. Preketes, A., Horton, M., Ross, W. and Morris, D. Hepatic cryotherapy: Double-freeze cycles achieve greater hepatocellular injury in man. *Cryobiology* **32**, 215-219 (1995).
8. Whittaker, D. Repeat freeze cycles in cryosurgery of oral tissues. *Brit. Dent. J.* **139**, 459-464 (1975).

9. Dilley, A., Dy, D., Warlters, A., Copeland, S., Gillies, A., Morris, R., Gibb, D., Cook, T., and Morris, D. Laboratory and animal model evaluation of the Cryotech LCS 2000 in hepatic cryotherapy. *Cryobiology* **30**, 74-85 (1993).

10. Homasson, J.P., Thiery, J.P., Angebault, M., Ovtracht, L., and Maiwand, O. The operation and efficacy of cryosurgical, nitrous oxide-driven cryoprobe I Cryoprobe physical characteristics: their effects on cell cryodestruction. *Cryobiology* **31**, 290-304 (1994).

11. BioSource International. AlamarBlue™ assay. Package insert.

12. Gage, A. Review: Mechanisms of tissue injury in cryosurgery. *Cryobiology* **37**, 171-186 (1998).

13. Gage, A., Guest, K., Montes, M., Caruana, J. and Whalen, D. Effect of varying freezing and thawing rates in experimental cryosurgery. *Cryobiology* **22**, 175-182 (1985).

14. Lovelock, J. The hemolysis of human red blood-cells by freezing and thawing. *Biochemica Et Biophysica Acta* **10**, 414-426 (1953).

15. Farrant, J. and Morris, G. Thermal shock and dilution shock as the causes of freezing injury. *Cryobiology* **10**, 134-140 (1973).

16. Zacharian, S. The observation of freeze-thaw cycles upon cancer cell suspensions. *J. Dermatol. Surg. Oncol.* **3**, 173-174 (1977).

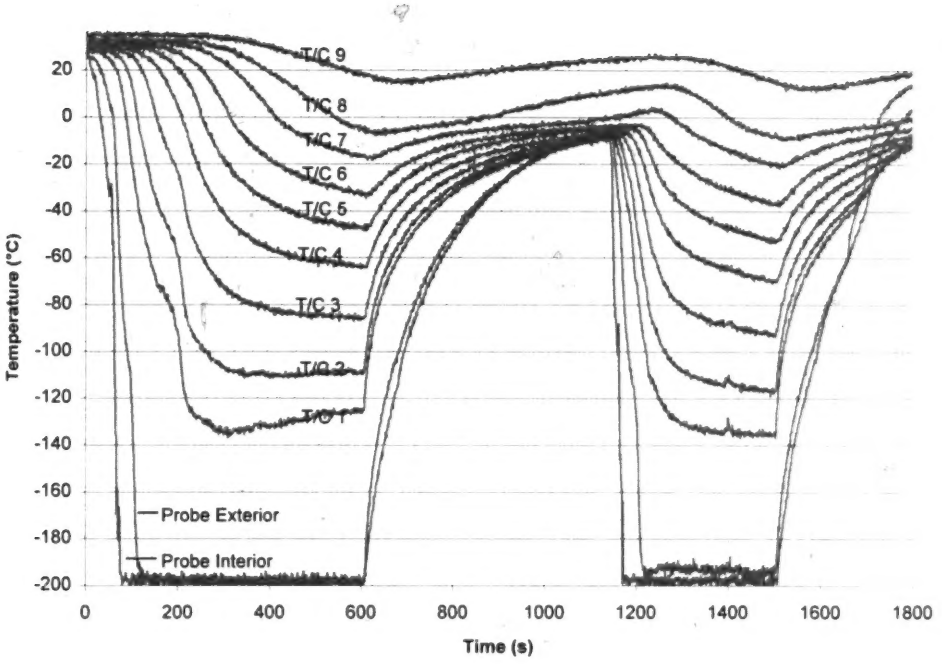

Figure 4.1 Example of a double freeze cycle protocol with cells. The temperature profiles correspond to thermocouple measurements taken in the chamber. The first two curves on the bottom of the graph represent the temperatures inside and outside the probe. The other curves are the freezing profiles of methocel with increasing distance from the probe.

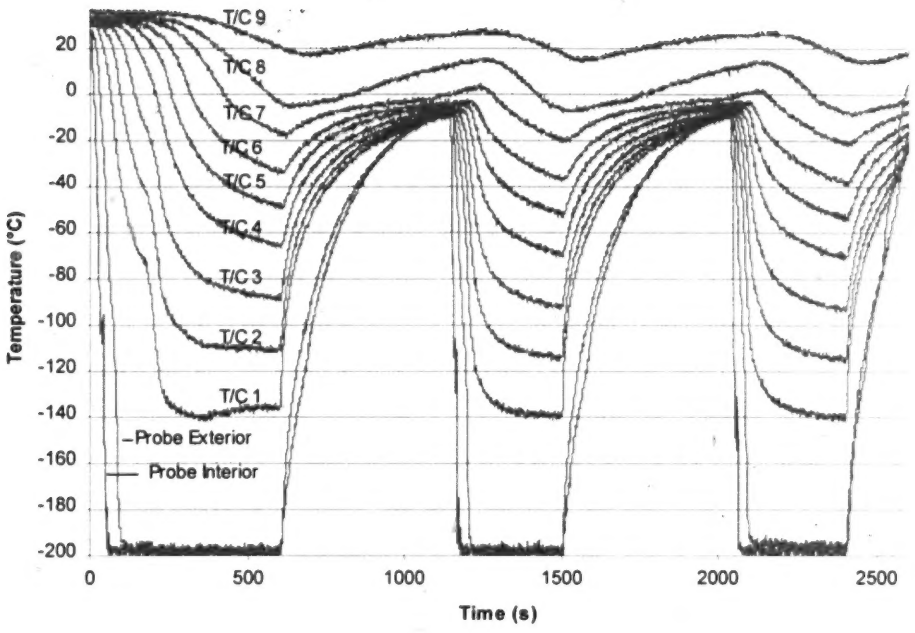

Figure 4.2 Example of a triple freeze cycle protocol with cells. The temperature profiles correspond to thermocouple measurements taken in the chamber. The first two curves on the bottom of the graph represent the temperatures inside and outside the probe. The other curves are the freezing profiles of methocel with increasing distance from the probe.

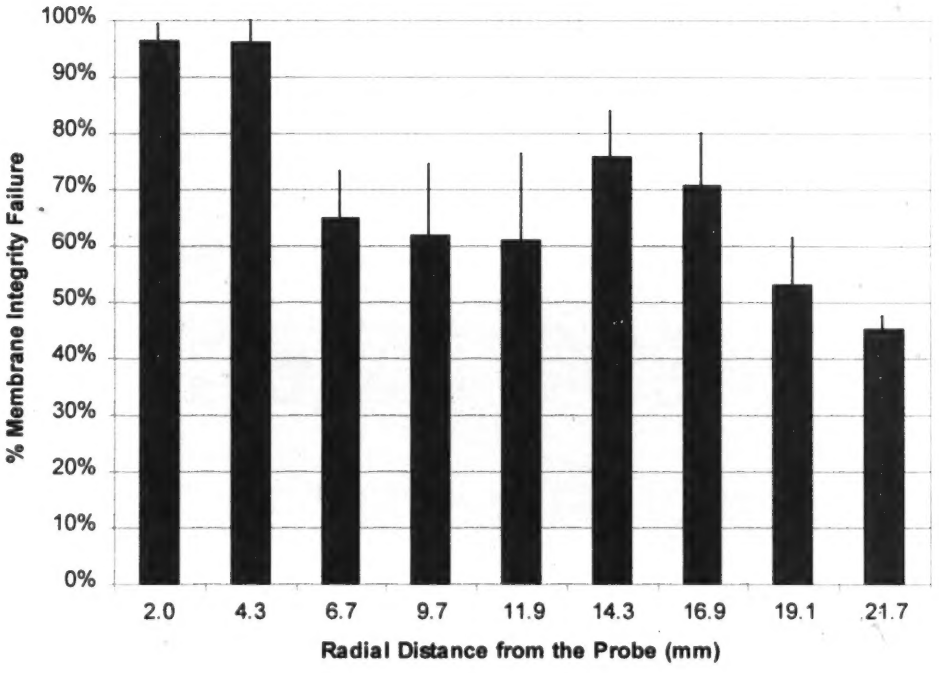

Figure 4.3 Membrane integrity staining results for the double freeze cycle protocol with respect to radial distance from the probe.

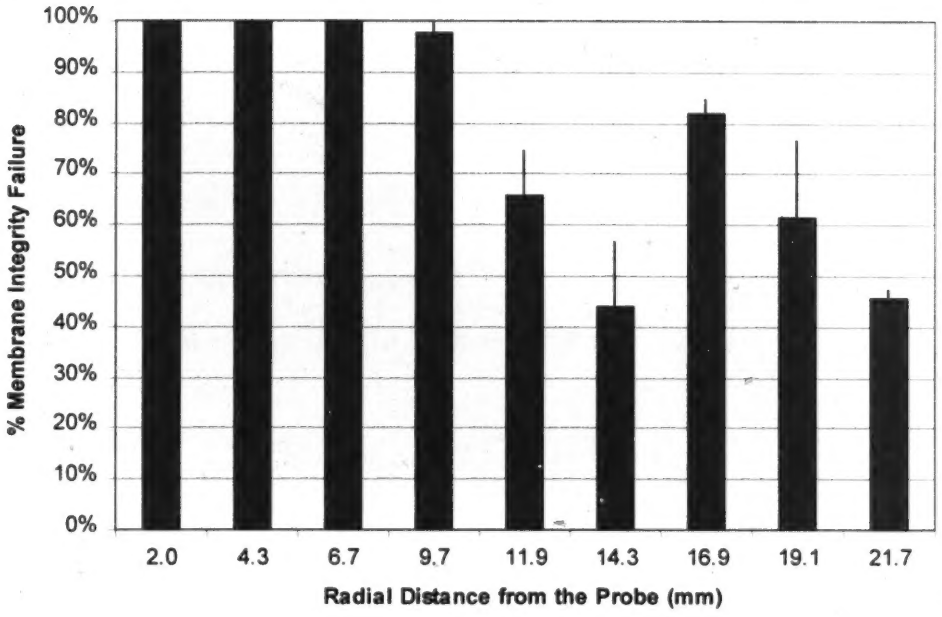

Figure 4.4 Membrane integrity staining results for the triple freeze cycle protocol with respect to radial distance from the probe.

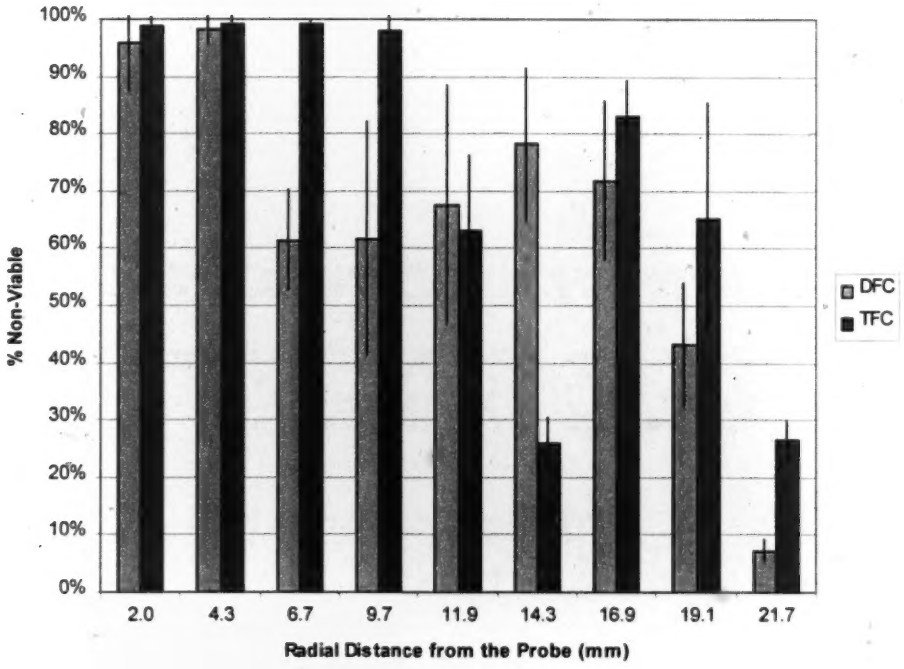

Figure 4.5 Comparison of cell viability for the double and triple freeze cycle protocols with respect to distance from the probe using alamarBlue, where DFC is the double freeze cycle and TFC is the triple freeze cycle.

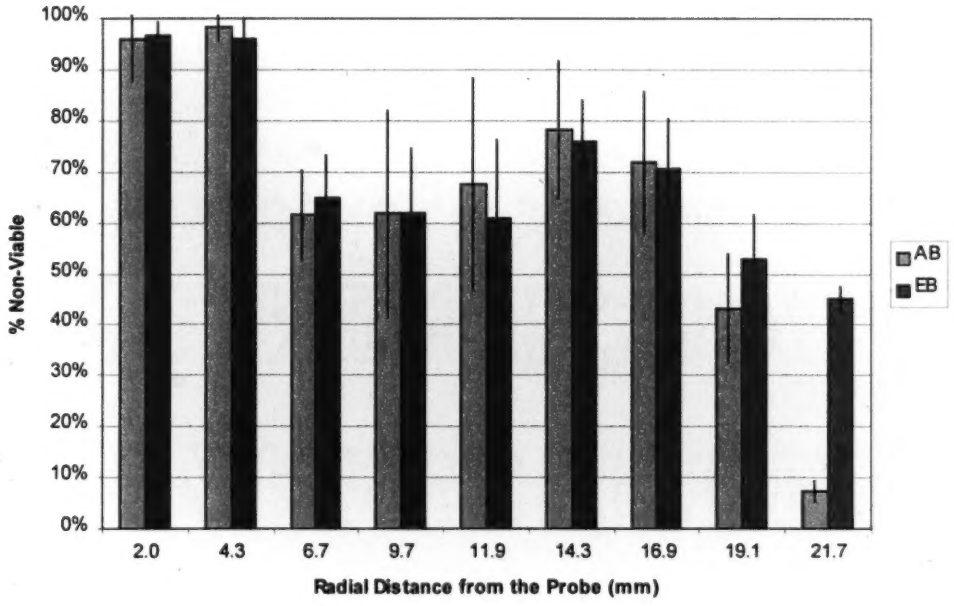

Figure 4.6 Viability comparison of Syto/EB versus alamarBlue at various distances from the probe for the double freeze cycle protocol.

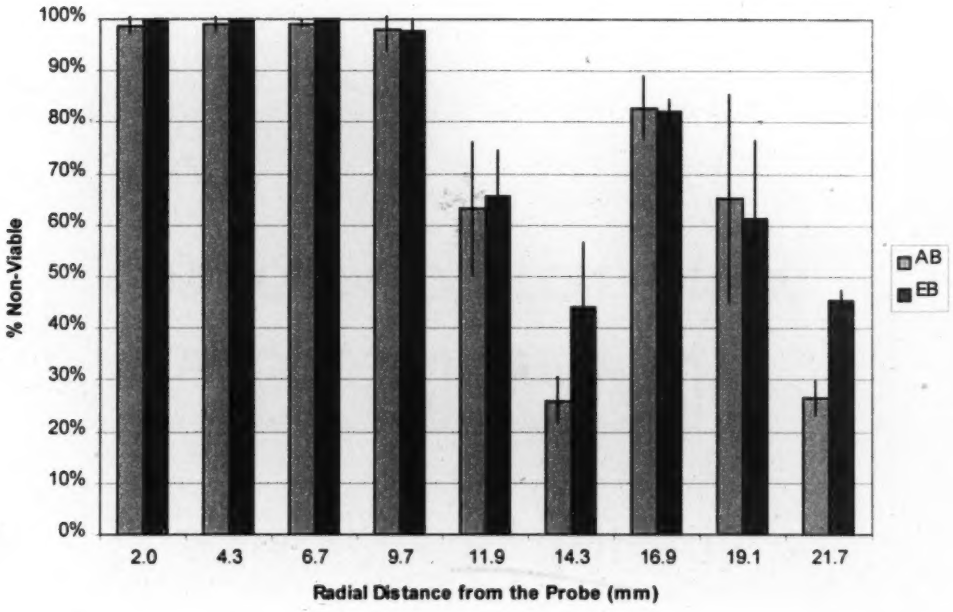

Figure 4.7 Viability comparison of Syto/EB versus alamarBlue at various distances from the probe in the triple freeze cycle protocol.

Radius (mm)	Double Freeze Cycle (% intact)	Triple Freeze Cycle (% intact)
2.0	4 ±3	0 ±0
4.3	4 ±4	0 ±0
6.7	35 ±8	0 ±0
9.7	38 ±13	2 ±2
11.9	39 ±15	34 ±9
14.3	24 ±8	56 ±13
16.9	29 ±9	18 ±2
19.1	47 ±9	38 ±15
21.7	55 ±2	55 ±2

Table 4.1 Comparison of Syto/EB results for the double and triple freeze cycle protocols with respect to distance from the probe.

Radius (mm)	Cell Death (%)	Cooling Rate 1 (°C/min)	Cooling Rate 2 (°C/min)
2.0	96 ±6	63	101
4.3	97 ±3	49	78
6.7	63 ±9	38	55
9.7	62 ±17	31	37
11.9	64 ±18	27	26
14.3	77 ±11	21	14
16.9	71 ±12	14	11
19.1	48 ±10	10	10
21.7	26 ±2	4	5

Table 4.2 The results of cooling rate (1 and 2 are the first and second freezes respectively) versus viability for the double freeze cycle protocol. Radius is the distance from the probe, cell death is the percent of non-viable cells represented by averages of Syto/EB and alamarBlue together.

Radius (mm)	Cell Death (%)	Cooling Rate1 (°C/min)	Cooling Rate2 (°C/min)	Cooling Rate3 (°C/min)
2.0	99 ±1	65	105	101
4.3	99 ±1	49	76	73
6.7	100 ±0	38	56	53
9.7	98 ±3	29	37	36
11.9	64 ±11	28	26	25
14.3	35 ±8	23	15	15
16.9	82 ±4	15	10	10
19.1	63 ±18	11	10	10
21.7	36 ±3	6	5	6

Table 4.3 The results of cooling rate versus viability for the triple freeze cycle protocol. Radius is the distance from the probe, cell death is the percent of non-viable cells represented by averages of Syto/EB and alamarBlue together. The numbers 1, 2, and 3 represent the first, second, and third freeze respectively.

Radius (mm)	Cell Death (%)	End Temperature 1 (°C)	End Temperature 2 (°C)
2.0	96 ±6	-136	-138
4.3	97 ±3	-108	-117
6.7	63 ±9	-83	-92
9.7	62 ±17	-61	-70
11.9	64 ±18	-46	-53
14.3	77 ±11	-31	-37
16.9	71 ±12	-16	-21
19.1	48 ±10	-5	-9
21.7	26 ±2	19	15

Table 4.4 The results of end temperature versus viability for the double freeze cycle protocol. Radius is the distance from the probe, cell death is the percent of non-viable cells represented by averages of Syto/EB and alamarBlue together. End temperatures 1 and 2 are the lowest temperatures reached during the first and second freeze respectively.

Radius (mm)	Cell Death (%)	End Temperature 1 (°C)	End Temperature 2 (°C)	End Temperature 3 (°C)
2.0	99 ±1	-142	-137	-139
4.3	99 ±1	-112	-113	-114
6.7	100 ±0	-89	-91	-93
9.7	98 ±3	-67	-70	-70
11.9	64 ±11	-51	-53	-54
14.3	35 ±8	-36	-39	-40
16.9	82 ±4	-20	-21	-21
19.1	63 ±18	-8	-9	-10
21.7	36 ±3	14	13	12

Table 4.5 The results of end temperature versus viability for the triple freeze cycle protocol. Radius is the distance from the probe, cell death is the percent of non-viable cells represented by averages of Syto/EB and alamarBlue together. End temperatures 1, 2 and 3 are the lowest temperatures reached during the first, second and third freeze respectively.

CHAPTER 5: GENERAL DISCUSSION AND CONCLUSIONS

5.1 Review of Thesis Objectives

The main objective of this research is a better understanding of the biological responses of tumour cells to freezing during cryosurgery. The tactics involved include; building a realistic cryosurgical model system that allows assessment of cryosurgical procedures, determination of adequate biological assessment techniques of the cells after freezing, and performance and analysis of freeze-thaw biological response experiments. The hypothesis is that the model system will permit correlation of physical and thermal measurements with biological outcomes, to assess and increase the efficiency of different cryotherapeutic protocols.

5.2 Summary of Results

The goal reached with this work is the development of an experimental model system that allows physical and thermal measurements to be correlated with biological outcomes. This was accomplished by designing a realistic cryosurgical model system. The system is validated in appendix A by the development of a combined theoretical and experimental model system to describe transient temperature profiles. The chamber provides a controlled environment for the assessment of biological outcomes of cryosurgical procedures. The model system enables exact temperature measurements and tissue biopsy sites within a tissue representative size system that has not been developed before.

Biological assessment techniques and a model tissue system are validated in chapter 2. Methocel is an excellent representative of a tissue system that allows the study of an intermediate step between that of real tissues and single cells in suspension. The advantage of using methocel is the ease in which samples can be biopsied and used in conjunction with the viability assessment techniques.

The relationship between cell viability and cryosurgical conditions during the freezing process is then investigated. The results of the single and double freeze-thaw protocols give a good indication of what happens to cells on a basic cryobiological level and as a result of freezing injury alone. It is quite evident that a single freeze-thaw is insufficient when considering this treatment for cancer due to the amounts of cell survival. The lack of damage in the outer portion of the ice-ball is very obvious and the simple task of performing a second freeze results in two fold increase in cell kill at the periphery of the ice-ball. This effect is more than likely a combination of many factors, which include the duration of freeze and being subjected twice to the same damaging events. The double freeze-thaw cycle is very efficient at killing cells both in the centre and periphery of the ice-ball but still allows some cells to survive.

Results of the temperature cycling experiments show that they are more effective at killing cells in the periphery of the ice-ball than the single freeze-thaw protocol. The double and triple freeze cycles do not kill more cells in the periphery of the ice-ball when compared to the double freeze-thaw protocol. The main difference in the cycling protocols is that complete thawing of the ice-ball

before refreezing is not performed. The importance of completely thawing the ice-ball in increasing the effectiveness of cryosurgery is well documented from these experiments. Complete thawing allows redistribution of water within cells and tissues, and results in dilution injury in both the frozen and unfrozen portions of the ice-ball. As a result of these experiments, more information is known about temperature cycling and its lack of efficiency at killing cells in the periphery of the ice-ball.

5.3 Significance to Cryosurgery

The results presented here represent direct freezing injury and do not incorporate damage that is contributed by secondary factors such as ischemia. What combination of these two factors contributes to 100% kill in the ice-ball remains unknown and requires further research. The double freeze-thaw is the most efficient of all protocols studied here and yet does not result in a cure clinically in many cases. Increasing the number of cycles is not possible due to the resultant complications. If cryosurgery is to result in 100% kill, research into adjuvant therapies should be performed so that the target rate of cell kill is reached.

APPENDIX A: VALIDATION OF AN EXPERIMENTAL MODEL SYSTEM FOR CRYOSURGERY

A.1 Introduction

Cryosurgery is being used with increasing frequency in the treatment of deep organ tumours, but the ability of some cells to survive freezing at low sub-zero temperatures prevents cure (1,2,3,4). A better understanding of cell and tissue responses to freezing is necessary to improve cell kill and increase the predictability of cryosurgery. Realising how freeze-thaw conditions affect biological outcomes of cryosurgical procedures will lead to improvements in treatment.

A more scientific approach to cryosurgery is necessary to standardise methods and make tumour cell kill reproducible. An experimental model system has been developed to allow physical and thermal measurements to be correlated with biological outcomes. The specific design objectives include: the system must be a physically realistic model of cryosurgery with well defined boundary conditions; it must allow assessment of cryosurgical procedures in a controlled environment to define more effective freeze-thaw protocols; it must be amenable to theoretical descriptions that correlate with experimental measurements in a reproducible manner to validate the model system and for future theoretical modeling of thermal and cryobiological responses; and it must allow correlation of thermal profiles and freezing conditions with biological outcomes that can be directly applied to improving treatment planning of cryosurgery.

In cryosurgery, the probe functions as a heat sink, removing heat by conduction from the tissue (5). Ice forms on the surface of the probe by addition of water molecules to the freezing front in the direction of the temperature gradient. Heat is transported by conduction heat transfer through the ice-ball into the probe (5). The cooling ability of the probe and conduction heat transfer through the frozen region both limit the amount of tissue that can be frozen. The increasing size of the ice-ball affects the ability of the probe to remove heat from the freezing interface. Blood perfusion and contributions from the surrounding metabolically active tissue add additional heat to the system and significantly affect the freezing process (5). From a theoretical perspective, it is possible to model this system using heat transfer energy equations in a radial co-ordinate direction. No new equations are derived in this chapter; they are based on heat transfer in an infinite cylinder (6), with approximation of ice-ball location using steady-state and transient ice front predictions. All theoretical predictions were derived and calculated by Dr. Rick Batycky and Mr. Roderick Gonzales of the Chemical Engineering Department at the University of Alberta.

Steady-state Ice Front Prediction

The location of the ice-ball can be theoretically calculated in this model system. In a one-phase model it is assumed that both ice and water have the same thermal properties, giving (eqn 1):

$$\frac{r_b}{r_1} = \left(\frac{r_2}{r_1}\right)^{\frac{T_b - T_1}{T_2 - T_1}}$$

where r_1 is the inner radius, r_2 is the outer radius, T_1 is the temperature at the probe, T_2 is the external temperature at the outside wall of the container, and T_b is the freezing point. If the values for r_1, r_2, T_1 and T_2 are known then it is possible to calculate r_b, the ice-ball radius.

However, if ice and water have different thermal conductivities, this must be taken into consideration during calculations. An important parameter appearing in this case is λ, the ratio of thermal conductivities k for each phase (eqn 2):

$$\lambda \overset{def}{=} \frac{k_{ice}}{k_{water}}$$

Different solutions arise when including λ, which takes into account the differences in thermal conductivities to give the equation (eqn 3)

$$\frac{r_b}{r_1} = \left(\frac{r_2}{r_1}\right)^{\frac{\lambda}{\frac{T_2-T_1}{T_b-T_1}-1+\lambda}}$$

For k_{ice} = 2.22 w/(mK) and k_{water} = 0.569 w/(mK), λ = 3.90. When considering experimental values in the equation, for example at T_1 = -195°C and T_2 = 17.3°C if we assume that the differences in thermal conductivities are insignificant then r_b forms 86% across. However, if the differences are important and the value for λ included, then theoretically the ice-ball will be 96% across.

These differences are not trivial in determining size of the ice-ball. So distinction between different thermal conductivities proves to be very significant. Due to the difference between experimental and theoretical sizes of the ice-ball,

this also suggests that the thermal properties of the probe must be taken into account and included in the equation.

Transient: Unsteady-state Single Phase

The equations governing heat transfer in a cylindrical steady-state apparatus in the absence of convection are (eqn 4):

$$\frac{\partial T}{\partial t} = \alpha\left(\frac{\partial^2 T}{\partial r^2} + \frac{1}{r}\frac{\partial T}{\partial r}\right)$$

where $\alpha = k/\rho c$ is the thermal diffusivity, ρ the density, and c the heat capacity. This must be solved subject to boundary conditions:

$T = T_1$ at $r = r_1$

$T = T_2$ at $r = r_2$

and initial conditions:

$T = T_2$ at $t = 0$

Using standard methods of separation of variables the solution for unsteady-state temperature is (eqn 5):

$$T = \pi \sum_{n=1}^{\infty} \frac{(T_1 - T_2)J_0(r_2\beta_n)J_0(r_1\beta_n)}{J_0^2(r_1\beta_n) - J_0^2(r_2\beta_n)} e^{-\alpha\beta_n^2 t} U_0(r\beta_n) + \frac{T_1 \ln(r_2/r) + T_2 \ln(r/r_1)}{\ln(r_2/r_1)}$$

where J_o is a Bessel function, β_n are eigenvalues, and U_o the eigenfunctions (7).

A.2 Methods and Materials

The following description of the cryosurgical model system is presented in figure A.1. The system consists of a disk shaped chamber in which the outer circumference and bottom are made out of Teflon™. The lid is comprised of

Plexiglas™ with small holes drilled through the top outward in the radial direction, slightly skewed from one another. The holes on opposite sides of the lid are located equidistant from one another so that point temperature measurements are at the same location as the samples removed from the chamber. The holes on one side will be used to biopsy biological samples from within the chamber and are large enough to accommodate 19 gauge 1½ inch (3.81 mm) needles (Becton Dickinson and Company, Franklin Lakes, NJ). The holes that are equidistant apart on the opposite side of the lid contain 0.01 inch (0.25 mm) T-type Teflon insulated thermocouples (OMEGA Engineering, Stamford, CT) that are used to measure temperatures profiles at specific locations within the sample. Data from the thermocouples is recorded by the DaqBook™ multichannel data acquisition system with DBK 19 thermocouple card (OMEGA Engineering) connected to a computer. The radius of the ice-ball is measured using a video recording of the freezing process. There are nine thermocouples penetrating the holes into the chamber that measure temperatures according to radius from the probe. One thermocouple is placed inside the probe to monitor probe interior temperatures at the level of ice-ball formation and compared to the probes actual temperature, measured by a thermocouple placed on the exterior of the probe just as it is exiting the chamber.

A stainless steel pipe of outer diameter 4.7 mm and thickness 0.75 mm functions as a cryoprobe and runs axially through the chamber. Stainless steel was chosen because of its relatively high thermal conductivity, capacity to avoid corrosion, and cost effectiveness. The probe is connected at both ends with

plastic insulated tubing that act as conduits for the liquid nitrogen inlet and outlet. A pressurized Dewar functions as a reservoir and source of liquid nitrogen, and excess liquid nitrogen is collected in an unpressurized collection Dewar.

In these experiments the experimental chamber contains distilled water, used to validate the known theoretical descriptions of freezing water with the actual experimental measurements. First a liquid nitrogen Dewar is filled and pressurized, then attached to the system. The lid with thermocouples is secured to the top of the system as soon as 30 ml of distilled water is added. Making sure that all the connections in the system are attached, the data acquisition system and liquid nitrogen source are activated simultaneously, marking the beginning of the freezing cycle. After 5 minutes the liquid nitrogen source is removed. The DaqBook temperature data is then analysed in Excel®. The on screen measurements of ice-ball radius taken by the video camera are converted into real measurements so that ice-ball radius vs. time information can be determined.

A.3 Results

The unsteady-state equation (eqn 5) is then used to derive the theoretical temperature profiles using the following assumptions: a) the circular experimental chamber containing the cooling water has a radius (r_2) of 30.3 mm and had insulated top and bottom b) the radius of the probe (r_1) is 4.7 mm and is maintained at –160°C (T_1) c) the outer insulated wall is maintained at 20°C.

A theoretical plot of temperature versus time for different radial distances from the probe is presented in figure A.2. The theoretical distance of the ice-ball

from the probe is calculated from the temperature profile of each thermocouple as it passes 0°C.

Theoretical and experimental thermal profile measurements from the system are compared in figure A.3. The model and experimental measurements look similar. There is a shift in each experimental temperature profile to the right of the theoretical curve at the beginning of the freeze. This shift is more noticeable in the profile further from the cryosurgical probe.

Figure A.4 compares the theoretical ice-ball radius from figure A.2 to the experimental ice-ball radius. The values are very similar, but a slight delay is seen in the beginning of the experimental curve. At the end of the curve, the experimental ice-ball is slightly larger than the theoretical.

A.4 Discussion

The comparison of the theoretical model and experimental temperatures in figure A.3 reveals that the analytical solution of the theoretical description of the system was validated using water. The two curves are very similar, except for the shift to the right of the experimental curves. This time delay in the experimental values can be explained by the cooling down of supply tubes upon start up of the experimental system. The probe is not cooled instantaneously as a result.

The same time delay is seen in the comparison of ice-ball radii in figure A.4, and for the same reason. The liquid nitrogen cools the tubes first, then the probe after a short delay. The ice-ball radii are the same, except at the end of the freeze. This may be attributed to the differences in thermal conductivity between

the ice and the water, and has an effect of the ice front position. The increase in thermal conductivity of the ice allows heat to be transferred faster to the probe and results in a faster growing ice-ball.

In conclusion it can be said that: a combined experimental and theoretical model system has been developed to describe the transient temperature profiles for use in cryosurgical procedures; the influence of the different thermal properties of ice and water must be taken into account in any theoretical model; The effects due to cooling the probe are manifested as a delay in temperature response; and the system provides a controlled environment for assessment of biological outcomes of cryosurgical procedures.

A.5 References

1. Chuang, C., Chu, C., Chiang, H. and Chou, C. Application of cryoablation in the management of prostate cancer. *Chang Gung Med. J.* **20**, 201-206 (1997).
2. Morris, D. Hepatic cryotherapy for cancer: A review and critique. *HPB Surgery* **9**:2, 118-120 (1996).
3. Ravikumar, T. Interstitial therapies for liver tumors. *Surg. Oncol. Clin. N. Amer.* **5**:2, 365-377 (1996).
4. Wong, W., Chinn, D., Chinn, M., Chinn, J., Tom, W. and Tom, W. Cryosurgery as a treatment for prostate carcinoma: results and complications. *Cancer* **79**:5, 963-974 (1997).
5. Rubinsky, B. Thermodynamics and heat transfer in cryosurgery. *In* "Percutaneous Prostate Cryoablation" (G. Onik, B. Rubinsky, G. Watson and R. Ablin, Eds.), pp. 69-77, Quality Medical Publishing, St. Louis, 1995.
6. Carslaw, H. and Jaeger, J. Conduction of heat in solids. Oxford University Press, 1959.
7. Batycky, R., Hammerstedt, R. and Edwards, D. Osmotically driven intracellular transport phenomena. In press.

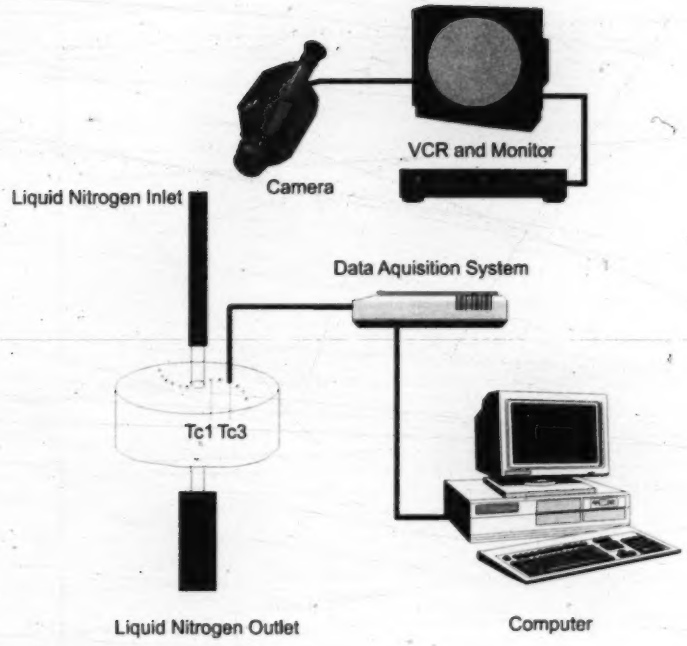

Figure A.1 Schematic of the cryosurgical model system.

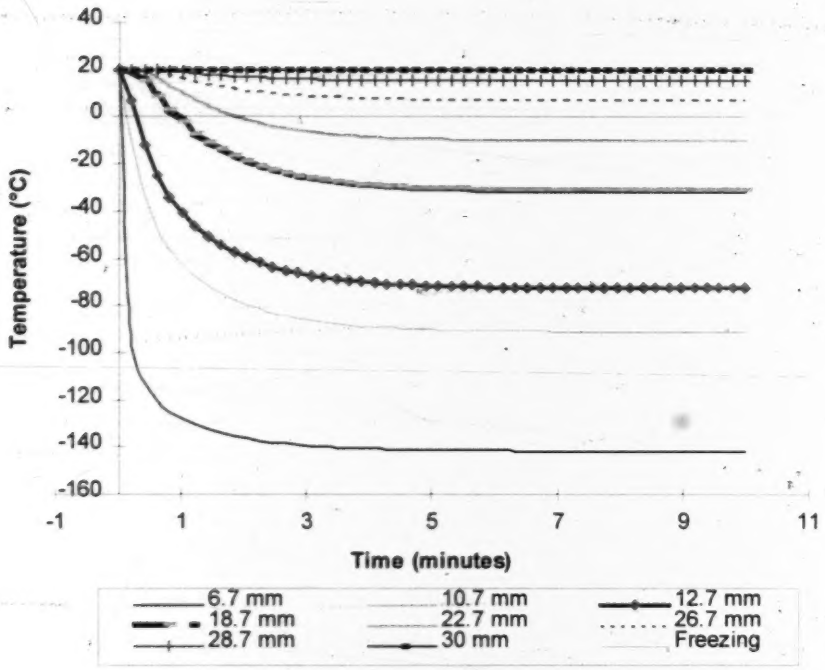

Figure A.2 Theoretical plot of temperature versus time for different radial distances from the probe.

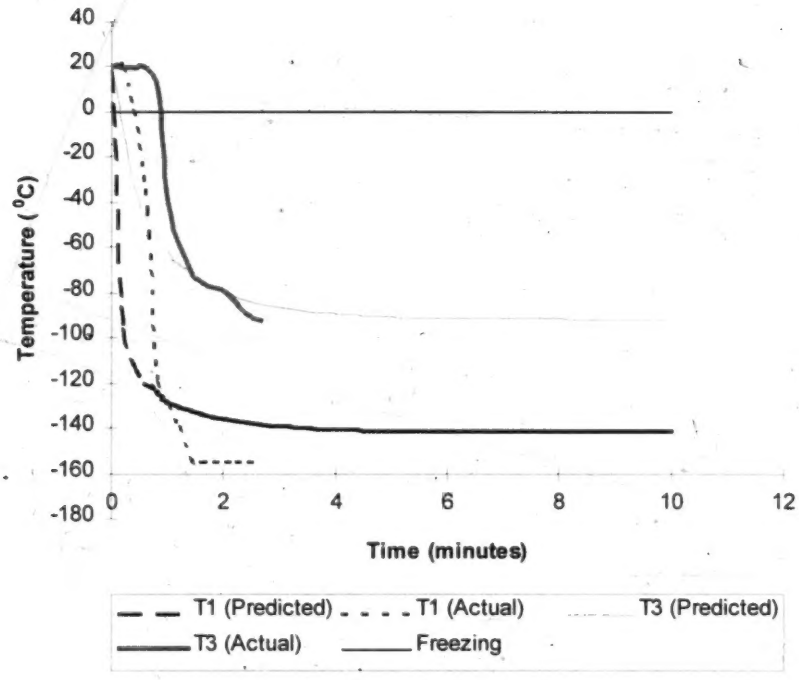

Figure A.3 Theoretical and experimental thermal profile measurements with respect to time.

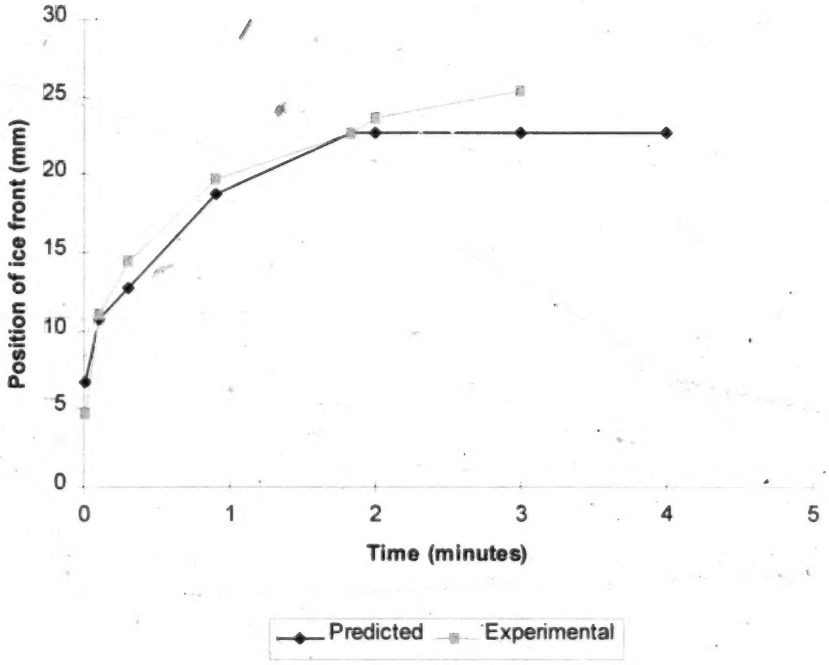

Figure A.4 Comparison of theoretical versus experimental ice-ball radius with respect to time.

APPENDIX B: ALAMARBLUE PERCENT REDUCTION EQUATION

B.1 General Discussion

AlamarBlue is an assay that detects metabolic activity of cells. AlamarBlue incorporates a REDOX indicator that changes colour in response to chemical reduction of the growth medium as a result of metabolism when it is reduced by cytochromes, $FMNH_2$, $FADH_2$, NADH, and NADPH (1). Changes in absorbance are used to determine the amounts of alamarBlue reduced. Equations have been developed to calculate the percent of alamarBlue reduced and include the absorbance at 570 and 600 nm. Initially, the reduction of alamarBlue was determined by subtracting the absorbance of alamarBlue at 600 nm from the absorbance of alamarBlue at 570 nm. This was found to be effective when the test wells were fully reacted. When the test wells are not fully reduced, there is an overlap in spectra due to the presence of the oxidized substrate at 570 nm. The manufacturer has provided an equation to calculate the amount of alamarBlue reduced that takes into account the overlap in spectra (1):

$$\%reduced = \frac{(117216)A_{570} - (80586)A_{600}}{(155677)A'_{600} - (14652)A'_{570}} \times 100 \qquad \text{(eqn1)}$$

where 117216 is the molar extinction coefficient of alamarBlue in the oxidized form at 600 nm, 80586 is the molar extinction coefficient of alamarBlue in the oxidized form at 570 nm, 14652 is the molar extinction coefficient of alamarBlue in the reduced form at 600 nm, 155677 is the molar extinction coefficient of alamarBlue in the reduced form at 570, A_{600} is the absorbance of the test wells at 600 nm, A_{570} is the absorbance of the test wells at 570 nm, A'_{600} is the

absorbance of the negative control wells at 600 nm, and A'_{570} is the absorbance of the negative control wells at 570 nm.

Equation 1 is used in the experiments in chapters 1, 2, and 3 to determine the percent of alamarBlue reduced. It has also been used successfully in another study where it is proven to be a simple and non-toxic assay to monitor cell viability *in vitro* (2).

B.2 References

1. BioSource International. AlamarBlue™ assay. Package insert.
2. Larson, E., Doughman, D., Gregerson, D., and Obritsch, W. A new, simple, nonradioactive, nontoxic in vitro assay to monitor corneal endothelial cell viability. *Invest. Ophthalmol. & Vis. Sci.* **38**:10, 1929-1933 (1997).